Contents lists available at ScienceDirect

Transportation Research Part C

journal homepage: www.elsevier.com

From free-route air traffic to an adapted dynamic main-flow system

Ingrid Gerdes *, Annette Temme, Michael Schultz

Institute of Flight Guidance, DLR Braunschweig, Germany

ARTICLE INFO

Keywords:
Intersection trajectory
Free route airspace
Free routing
Trajectory clustering
Main-flow system

ABSTRACT

At present, en-route flight traffic is carried out on a system of predefined routes with a low number of intersections between aircraft trajectories. This enables the air traffic controllers to control and supervise the traffic, especially around these intersections. Consequently, the route system leads to a low ratio of used to unused airspace, where not necessarily the shortest route is used for each flight. To reduce trajectory length, the idea of free routing has been developed, whereby each aircraft uses the direct connection between origin and destination airport, generating a traffic distribution which uses nearly the entire available airspace. As a consequence, many intersections between flight trajectories occur, making it more difficult for controllers to handle. We use these intersections as the basis of a so-called main-flow system with trajectories consisting of intersection points instead of waypoints. The intersections of all trajectories of a traffic sample are clustered and the resulting cluster centres are used as nodes in a route system. Additional processing is applied to identify a system of main flows and reduce the number of intersections to an acceptable amount. Our approach is able to identify major traffic flows within unstructured great-circle traffic and to create a main-flow system which is a compromise between the flexibility of free routing and the easier surveillance by controllers in the case of a predefined route network. To prove the ability of the proposed method to identify main flows, it was applied to a scenario of planned flights following the standard route structure. Subsequent tests with two different free-routing scenarios led to new route systems where the median adapted trajectory length for flights of the traffic sample is merely 0.9% (respectively 4.1%) higher than the direct connections. Furthermore, structural complexity is lower for intersections (cluster centres) of the new main-flow system compared to those of direct or great-circle scenarios.

1. Introduction

The introduction of free routing has been under discussion for many years; see e.g. Airspace, 2017. Eurocontrol and ICAO (ICAO, 2017) provided a concept that was integrated in route-network guidelines (EUROCONTROL, 2017) and improvement plans (EUROCONTROL, 2018a). However, the free-routing concept has not yet been applied in areas with dense traffic, due to an increased controller workload caused by less structured traffic flows.

* Corresponding author.
E-mail addresses: ingrid.gerdes@dlr.de (I. Gerdes); annette.temme@dlr.de (A. Temme); michael.schultz@dlr.de (M. Schultz)

https://doi.org/10.1016/j.trc.2020.102633
Received 26 March 2019; Received in revised form 6 Febraury 2020; Accepted 25 March 2020
Available online xxx
0968-090/

ICAO's European airspace design section ICAO EUR/NAT Office, 2018 defines Free Route Airspace as follows:

> ***Free Route Airspace*** *(FRA) is a specified airspace within which users may freely plan a route between a defined entry point and a defined exit point, with the possibility to route via intermediate (published or unpublished) waypoints, without reference to the ATS route network, subject to airspace availability. Within this airspace, flights remain subject to air traffic control.*

On the contrary, in the case of free flight Hoekstra et al., 2000; Hoekstra, 2001, the pilot is completely responsible for conducting the flight, including selection of the flight route and maintaining the necessary separation. Simulations of free-route airspace have been conducted for regions with less complex traffic situations or artificial structures in Krzyzanowski, 2013; Sunil et al., 2016 and were restricted to upper airspace regions. An application of the concept in dense traffic regions is still open. An important point - especially when coping with dense traffic regions - is whether free routing implies unstructured traffic flows. Taking into account that all aircraft have to depart and land at airports, the positions of these airports and the scheduled flights between them limit the number of possible trajectories. Therefore, our approach is to restrict free routing to an appropriate system of main flows, i.e. routes with a high amount of traffic, and adapt each free-routing trajectory to match these flows. This main-flow system is created dynamically and relies on the actual traffic demand to offer the best possible adaptation for the actual traffic distribution. It can be seen as a slightly adapted free-routing approach.

The objective of our research is to provide a first approach for a better utilisation of the airspace without decreasing the level of structuring. The structure today is the backbone for airspace controllers to manage regions with dense traffic. Most approaches feature either a free-routing airspace or a structured one. In this paper, we combine both in order to investigate whether standard free routing is beneficial compared to free routing combined with a traffic-dependent, predefined route system. Marzuoli et al. (2014) stated that trajectory clustering can be used for traffic-flow management and that flows are more predictable and robust than traffic which is based on single aircraft. Such a combination could be especially helpful for airspace regions with higher traffic in order to ensure a manageable amount of workload and thus ensure the obligatory level of safety Sunil, 2019. A main problem of standard free routing in comparison to predefined routing structures is the increase of possible intersections between flight trajectories. The necessity to observe all flights and to ensure the mandatory separation between aircraft increases the complexity of air traffic management. The observation of a large number of possible intersections by airspace controllers would result in a considerable increase in workload. On the other hand, conflicts are less likely because the traffic is distributed over a wider part of the airspace. Therefore, a compromise has to be found between complexity and efficiency. The target of the presented research is to create a system which combines the benefits of free-routing trajectories with the smaller complexity of a predefined route system.

Within our approach, a system of main flows based on flights using free routing is created and applied as basis for an adaptable network of flow-centric routes. These main-flow routes are created dynamically based on a selected - e.g. daily - traffic sample. For the sample, flight trajectories are not considered as a sequence of waypoints with a certain time frequency. Instead, for each trajectory the intersection points with all other trajectories are calculated (Fig. 1) and ordered depending on distance to the origin for

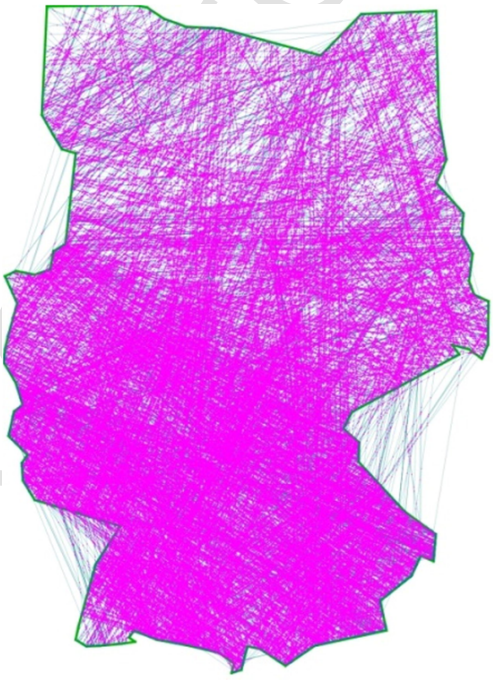

Fig. 1. Example of intersections as purple dots between great-circle trajectories (blue lines) within the German airspace boundary (flight level 320 and above).

each flight. Afterwards, the free-routing trajectory is substituted by the sequence of links between these intersection points. We call the resulting trajectory *"intersection trajectory"*.

The most important points besides the turning points featured in Gariel et al., 2011 are the intersection points among the trajectories when aggregating free-routing trajectories to a route network. Here, the intersection points are clustered to identify those points in the airspace where most trajectories intersect. These points are the edges of a graph system representing the underlying flight route system.

By applying clustering and optimisation techniques to the set of all intersection points, it is possible to analyse the structure of the traffic and to create an appropriate network of typical flight routes. By clustering similar flights into main flows – or sub-trajectories, see Lee et al., 2007 – an efficiently reduced main-flow system is created and the specific intersection trajectories are adjusted to this new main-flow system.

With this method, the traffic is merged into a set of main flows, which map the general traffic structure. To prove the feasibility of the proposed approach as regards creating an appropriate main-flow network, a baseline scenario was defined consisting of the last filed flight plans representing flight intentions without taking directs given by controllers into account. Subsequently, two free-routing scenarios with different traffic parameters were defined, simulated, compared and analysed. The focus is on efficiency measured by setting the trajectory length in relation to the direct connection and complexity by analysing the distribution of cluster centres and the connected link structure representing the main-flow intersections and their traffic load.

The paper is structured as follows: An overview of related work and methods applied is provided in Section 2.1. A brief summary of the mathematical background is given in Section 2.2. The general approach, together with all steps to build the identified main routes, is described in Section 3. Section 4 contains assumptions and limitations and in Section 5, the simulation setup with its traffic scenarios and simulation parameters is described. The results of the simulations of all scenarios are presented in Section 6 and compared and discussed in Section 7.

2. Background

2.1. Status quo

The idea of free flight became popular in the 1990s when several researchers developed its basics. Just like standard flight routes, free-flight trajectories have to be feasible and focused on safety, economic, and political constraints Hoekstra et al., 2000; Hoekstra, 2001. Conflict-free and efficient flight-route planning are discussed in Krzyzanowski, 2013, whilst Ratcliffe (2001) focuses on conflict-detection and avoidance mechanisms.

Here, we create a route system based on a given set of flight trajectories in free-route airspace. A straightforward approach to this problem is to identify those parts of the airspace which are used quite often and by a higher number of aircraft. In the literature, this is carried out with different approaches, e.g. by clustering trajectories or identifying and clustering segments of trajectories.

In the case of trajectory clustering, complete trajectories are considered and similar ones are grouped together Basora et al., 2017; Delahaye et al., 2018; Marzuoli et al., 2014. With such an approach, it is possible to distinguish between routes with different origin or destination even in the case of overlapping segments. This is used to identify and analyse traffic flows in controller-support tools. To create an artificial route network, segments of trajectories that several trajectories have in common are identified. For this, turning points of flights are identified and used as waypoints Gariel et al., 2011; Lee et al., 2007. In the case of arrival or departure routes, some segments of these routes are used as special link to, respectively from certain directions and some are common for all routes (e.g. glide path). The approach presented in Marzuoli et al., 2014 uses a two-step approach of clustering and a shortest-path algorithm to optimise flight trajectories. Here, we use similar steps to create a new airspace structure. Murca et al. (2016) generate a compact representation of daily traffic patterns in three steps. Firstly, artificial, equidistant trajectory waypoints are clustered to identify the major flight-trajectory pattern. Secondly, new trajectories are assigned to the appropriate pattern and outliers are detected. In the last step, operational Resource Use Patterns (RUP) for certain combinations of high, medium and low arrival and departure traffic are extracted. Churchill and Bloem (2019) used DBSCAN to cluster whole trajectories and to create a median trajectory (cluster centroid) as representative. They use a two-step approach: At first the trajectories are clustered with respect to their 2D shapes and afterwards in dependence on time.

An important point for all trajectory-clustering approaches is the selection of an appropriate similarity measure to compare trajectories or trajectory segments. Over the last years, many metrics were proposed and tested. Among the most common described in Yuan et al., 2017; Besse et al., 2016 are Euclidian, Haussdorff, Frechet and "Longest Common Sub-Sequence Metric (LCSS)" developed by Vlachos et al., 2002. A more recent metric called "Symmetrized Segment-Path Distance (SSPD)" was developed by Besse et al., 2016 and applied by Basora et al., 2017.

The clustering algorithms used can be divided into several groups, such as partition/distance-based clustering, density-based clustering Lee et al., 2007; Yuan et al., 2017 or hierarchical clustering such as HDBSCAN Mc Innes and Healy, 2017. Examples for distance-based clustering are the well-known k-means algorithm and its variants Mirkin, 1996. For density-based clustering, several algorithms based on DBSCAN (Density-Based Spatial Clustering of Applications with Noise) Ester et al., 1996 are widespread. Spectral clustering von Luxburg, 2007 or OPTICS Algorithm Ankerst et al., 1999 are other density-based clustering algorithms showing good results in the case of data sets with varying densities.

The trajectory-clustering methods listed above are not limited to flight trajectories but include taxi trajectories Besse et al., 2016; Churchill and Bloem, 2019, hurricane movements Lee, Han and Whang, 2007 or even deer movements and eye-tracking trajectories Vlachos et al., 2002. Furthermore, different approaches to identify popular routes from trajectories are carried out, e.g. with Markov chains Chen et al., 2011 that create a transfer network.

Sridhar et al. (2006) developed a tube network between clustered airports to profit from this reduced number of entry and exit points into the airspace system. In Xue and Kopardekar, 2009, tubes are identified based on clustering great-circle routes using the Hough transform. The identified tubes are seen as the basis for a network accommodating significant flights. In addition, special trajectory specifications caused e.g. by the usage of jet streams, severe weather conditions and airline operations (cost index Cook et al., 2009) are considered in a free-flight environment. Yousefi and Zadeh (2013) analysed the advantages of using corridors (Corridors-in-the-Sky, NextGen) for flights in certain directions to increase airspace capacity and to minimise interference from crossing traffic. Another approach to collecting and guiding parts of air traffic with common performance and similar direction was carried out by EUROCONTROL (2005), in which a freeway system with main directions and entry/exit points for leaving or entering these flows was defined resembling motorway traffic.

2.2. Methodological foundations

Here, we use the DBSCAN algorithm Ester et al., 1996 for the clustering tasks and A* as pathfinding algorithm Hart et al., 1968 to optimise the trajectories. To fine-tune the main-flow structure, a hill-climbing algorithm is applied. All three algorithms are described briefly below.

2.2.1. Clustering algorithm DBSCAN

The DBSCAN algorithm Ester et al., 1996; Besse et al., 2016 is a density-based algorithm which forms clusters based on the distribution of data in space. It groups together data points that are close to each other in relation to a given distance parameter ε. A data point is defined as element of a dense region when the number of data points with a distance less than or equal to ε exceeds a given minimum element number *minPts*.

Starting from a given point p, all elements q within distance ε of point p are counted. If the number is greater than or equal to *minPts*, p is a core object for a cluster. If a point q of this group has again at least *minPts* elements within the prescribed distance ε,q is called "directly density-reachable" from p. A point q' is called "density-reachable" from point p if there is a chain of points $q_1, \cdots, q_n$ with $p = q_1$. and $q' = q_n$ where q_{i+1} is directly density-reachable from q_i for all $i \in \{1, \cdots, n-1\}$. It can be seen as an element of the transitive hull of a cluster.

For the creation of a cluster, a first element with at least *minPts* points within its ε neighbourhood is selected as first element for a cluster. This cluster is expanded by adding all points in the ε neighbourhood of the first element as well as all elements inside the dense regions of these points (if they exist) to the actual cluster. This procedure is then repeated with an element not yet assigned to a cluster, until all elements are examined. Elements which have no dense region, respectively cluster they belong to are called noise. An advantage of DBSCAN is that it is not necessary to know the number of expected cluster centres in advance, as is the case for the k-means algorithm, see e.g. Mirkin, 1996.

2.2.2. Pathfinding algorithm A*

The A* algorithm Hart et al., 1968 is a generalisation of the Dijkstra algorithm. It was developed as a pathfinding algorithm with the goal of finding the shortest path by using problem-dependent information to estimate path costs. It operates on a weighted graph where the sum of cost (e.g. edge length) counted by moving through the network from a given origin to a destination is used as objective function. This algorithm tries to test those nodes first which seem to be most promising, e.g. because they are very close. For each possible node, the cost of reaching this node from the origin plus the estimated cost of moving from this node to the destination are calculated. For the second part, the direct connection from the observed point to the destination can be used as estimation. This is carried out until the destination is reached.

2.2.3. Hill-climbing algorithm

The hill-climbing algorithm is a mathematical optimisation technique with a focus on local search. It is an iterative algorithm that starts with an arbitrary problem solution s and then tries to find a better solution s' by making an incremental change to solution s. If the new solution is better than the last one, it is stored as current solution. These incremental changes are made to the actual solution until no further improvements can be found. The disadvantage of this method is that the search may stop in a local optimum instead of the global one. A termination criterion in the form of maximal steps is used to guarantee a predictable run-time.

3. General approach

This section describes the process of merging free-routing trajectories into main flows and the associated algorithm structure. The algorithm consists of a pre-processing and three main steps to calculate and improve the solution found by the first clustering process.

3.1. Pre-proccessing:

In a first step, entry and exit points at the selected airspace boundary for all trajectories are clustered to identify the beginnings or endings of the main-flow segments (Fig. 2). This is carried out with DBSCAN Ester et al., 1996. We used this type of algorithm as a first approach because it is able to handle non-convex cluster shapes. First tests with different types of cluster algorithms (DBSCAN, k-means) showed the necessity of using such an algorithm. Other density-based cluster algorithms will be part of our future research, including their computational performance. As metric, the Euclidian distance is used with nautical miles [NM as unit, which is a standard combination for measuring distances and determines conflicts between aircraft in ATM. The density is calculated in dependence on two parameters (Section 2.2.1). Outliers/noise, i.e. points not assigned to a cluster, are assigned to the closest boundary entry/exit cluster. All flight trajectories start, respectively end at the closest identified cluster. For entries/exits on the boundary, it is assumed that the trajectory starts/ends directly at these centre points, whilst for cluster centres inside the boundary, a link is added from the cluster centre to the real waypoint. This is done because these points may mark airports within the boundary.

In the next step, the intersection points between all free-routing trajectories are calculated for a predefined time period (Fig. 1). For each flight, the list of intersections is ordered chronologically. Thus, a so-called intersection trajectory consisting of links between intersections is constructed. The generated free-flight samples for the German airspace area have between 1.3 and 1.9 billion intersections. Due to the high number of trajectories per day, strategies to reduce the number of intersections are considered. Duplicate and similar intersections with a distance of less than 0.1 NM are identified and combined to one representative intersection, together with the number of duplicates.

The intersection points calculated in the pre-processing step A can be interpreted as zones of possible conflicts because many trajectories from different directions may use the same points. The presence of true conflicts depends on whether two aircraft will arrive at approximately the same time. To identify the general route structure and thereby the main-flow structure, the course of a flight route is the most important aspect, not the time when an aircraft reaches a specific point.

3.2. Main-flow processing:

After the identification of intersection points, these points are clustered using DBSCAN as density-based clustering algorithm and the Euclidian distance metric. A cluster centre is calculated as representative for each cluster, which is not necessarily convex. In tests with a k-means algorithm Mirkin, 1996, the cluster centres tended to be distributed equally like a grid over the observed airspace and did not reflect main flows.

A sequence of intersection points represents the trajectories. Therefore, those identified as noise by the DBSCAN must be handled to ensure that an appropriate cluster is associated with each intersection. Each noise point is assigned to the nearest cluster in a first approach. Tests with different parameter sets for a free-route sample with traffic within Germany have shown that selecting a set in which nearly all points belong to clusters leads to a few very big clusters which include the main portion of the data. Accordingly, the number of clusters is too low to identify the underlying traffic structure. In addition, there would be a high amount of intercepting trajectories increasing the pressure on highly frequented cluster centres and the possibility of conflicts. Therefore, the parameters for the DBSCAN have to be selected carefully (see Section 5). Due to the irregular shape of clusters, a free-routing trajectory may cross a large cluster multiple times. If non-consecutive intersections within a trajectory are associated with the same cluster, this may increase the trajectory length considerably (Fig. 3, left).

The mapping of intersection points to clusters may result e.g. in the following intersection trajectory: cluster1, cluster1, cluster2, cluster1, cluster1, cluster3. Therefore, for all flights, multiple intersections with the same clusters are removed from the intersection trajectories. In the example, the resulting intersection trajectory would be: cluster1, cluster2, cluster3; see Fig. 3.

To build the main-flow structure, an array consisting of $n_i * n_i$ elements, with $n_i, i \in \{A, O, R\}$ denoting the amount of cluster centres for adapted (A), optimised (O) and reduced (R) main-flow system, is created (Fig. 4). In this array, the number of flights between the corresponding cluster centres is stored based on the selected flight sample. The connection arrays of flight trajectories can be interpreted as lists of all allowed connections between cluster centres and can be used to calculate the main flows.

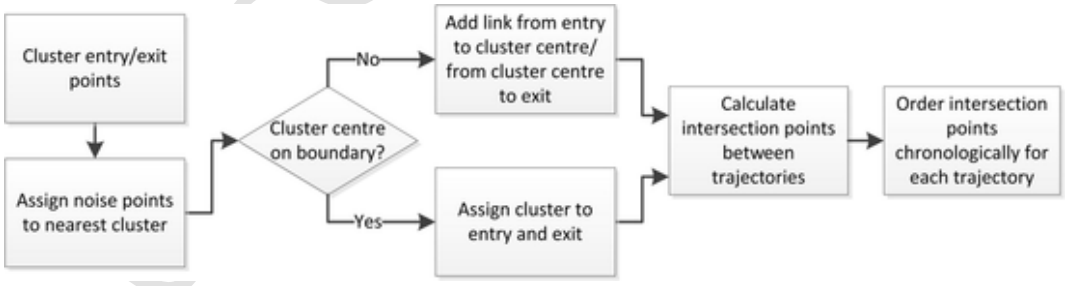

Fig. 2. Flow diagram pre-processing.

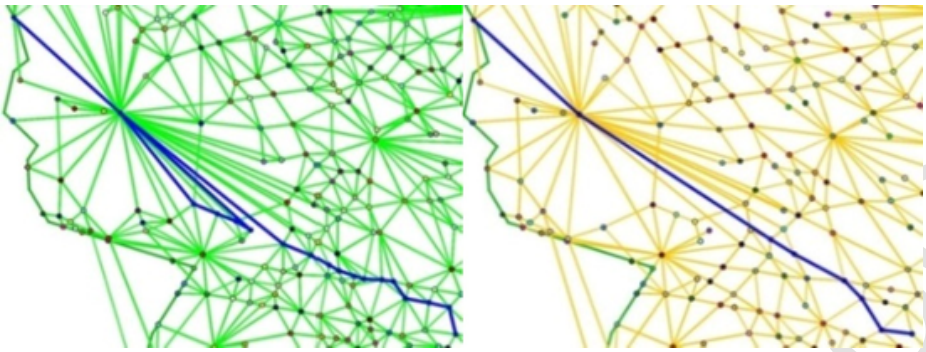

Fig. 3. Flight trajectory as sequence of clusters (boundary in dark green). Left: Trajectory after first step (allowed links in green). Right: Trajectory optimised with A* on reduced cluster system (allowed links in yellow). (For interpretation of the references to colour in this figure legend, the reader is referred to the web version of this article.)

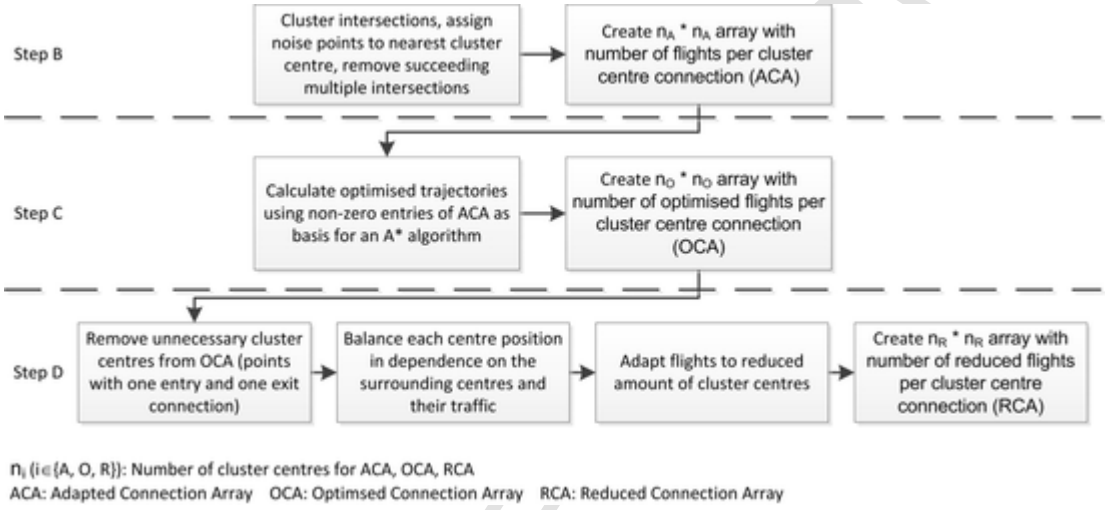

Fig. 4. Flow diagram main-flow creation.

The association of intersection points of each trajectory with the appropriate cluster centres may lead to routes which are longer than necessary. Therefore, the shortest route in the main-flow system defined by the ACA is calculated with a pathfinding A* algorithm. As basis for this A* algorithm, an interpretation of the ACA is used whereby each combination of cluster centres with an entry greater than zero marks an allowed edge. Again, a connection array for these optimised trajectories is determined (Optimised Connection Array: OCA). In the next step, nodes with only two connected links (one entry, one exit) are substituted by a single link between the surrounding cluster nodes. This procedure is not applied to cluster centres which are entries or exits of flight trajectories. In the example in Fig. 5, the orange cluster centre and the connections are removed and replaced by the red line.

The next step is a slight adaptation to smooth main flows used by many flights and to decrease the average length of the most frequented main flows. The aim is to position a cluster centre in order to minimise the length of subsequent links used in trajectories (Fig. 6, left) moving through this centre. This length, together with the number of flights using these subsequent links, is used with hill climbing (Section 2.2.3) to optimise the centre position. Hill climbing is restricted to the vicinity of the old centre coordinates with a maximal distance of 2.5 NM, shown as a green circle in Fig. 6. Because of the restriction to a small area around the original position, the optimisation is performed for each cluster centre separately.

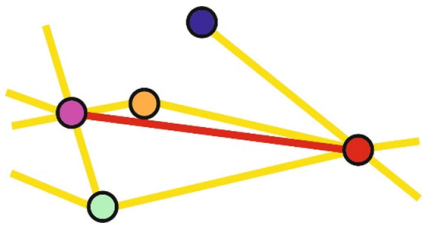

Fig. 5. Removing redundant cluster centres.

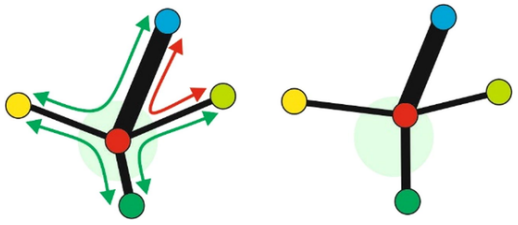

Fig. 6. Point balancing example. Green arrows: used segment combination, red: unused segment combination, green circle: reposition area. (For interpretation of the references to colour in this figure legend, the reader is referred to the web version of this article.)

This can be formalised as follows: Let $S_{EL}(c)$ be the set of segment combinations entering ($\overline{pc}$) and leaving ($\overline{cq}$) a selected cluster centre c.Then, the position of c is balanced with respect to the weighted sum of subsequent link lengths of the elements $s_{pq} \in S_{EL}(c)$ for each cluster centre c. The weights are the number of flights n_{pq} using the corresponding subsequent links. The resulting evaluation function $eval(c^*)$, which has to be minimised, has the following form:

$$eval\,(c^*) = \sum_{s_{pq} \in S_{EL}(c)} \left(\sqrt{\left((p_x - c_x^*)^2 + (p_y - c_y^*)^2\right)} + \sqrt{\left((c_x^* - q_x)^2 + (c_y^* - q_y)^2\right)} \right) * n_{pq} \tag{1}$$

$$\text{with} \quad \sqrt{\left((c_x^* - c_x)^2 + (c_y^* - c_y)^2\right)} < 2.5 \tag{2}$$

Subsequently, a new connection array is created for the reduced main-flow system (Reduced Connection Array: RCA).
The described algorithm has the following structure divided into four main steps:

Step A: Pre-processing:
1. Clustering of entry and exit points to the selected airspace for all flights of the flight sample using DBSCAN.
2. Calculation of all intersection points between all flight trajectories in the scenario disregarding flight times.
3. Sort intersection list for each flight depending on time in ascending order.

Step B: Creation of Adapted Main-Flow System
Calculate cluster centres for intersections using DBSCAN.
Assign nearest cluster centre to intersections marked as noise.
In the case of consecutive multiple intersections with the same cluster, remove all but the first one.
Create connection array for adapted main-flow system (ACA) containing the number of flights using the connection.

Step C: Creation of Optimised Main-Flow System
1. Use A* pathfinding algorithm to identify the shortest connection between entry and exit point for each flight using ACA.
2. Create connection array for optimised main-flow system (OCA).

Step D: Creation of Reduced Main-Flow System
1. Identify all combinations of three consecutive linked cluster centres where the middle centre has no other links and is therefore obsolete. Remove these nodes.
2. Adapt intersection list of flights accordingly.
3. Balance the positions of all cluster centres with respect to the sum of distances to the connected cluster centres using hill climbing.
4. Create connection array for reduced main-flow system (RCA).

4. Assumptions and limitations

The target of our approach is to create a basic en-route system of route designators (cluster centres) and connecting routes similar to those used today (see e.g. AIP Germany, ENR 3.3 RNAV Routes). The constructed main-flow system consists of bidirectional connections between clusters. To separate traffic with different flight directions, semi-circular cruising levels can be applied to the created main-flow system to separate traffic with opposite flight directions. This follows the definition of route designators in the AIP where many designators use odd/even flight levels for different flight directions. Nevertheless, route designators limited to one direction exist as well. The limitation to airspace above flight level 320 reduces the amount of climbing and descending traffic that could otherwise disturb the flight level system depending on flight directions. Since the main-flow system is based on planned traffic above flight level 320, directional restrictions are automatically transferred to it. For an application of this method to lower flight levels or a TMA, considering directions would allow the flows to separate arriving and departing traffic (as is done today by using SIDs and STARs).

Every entry/exit will be assigned to an appropriate entry/exit cluster. Especially in the case of direct flights created by using the great circle between start and destination airport, it is possible that there is a considerable distance between the original entry/exit

point and the assigned cluster centre. It is assumed that all aircraft will fly direct to their sector entry point and will resume their normal route when exiting the sector.

Another important assumption is to neglect the actual flight times when calculating the intersections between flight trajectories. This is done because the focus of the approach presented here lies on the creation of a route structure with characteristic crossing points, not on identifying conflicts or creating new flight routes based on the main-flow system. Furthermore, in the case of planned flights, the flight times are not reliable. For direct routes, only the entry time is known from the original flight; speeds and used flight level have to be estimated based on the original (planned) data. Therefore, the intersection points are interpreted as traffic crossing rather than possible conflict zones between two aircraft. For the same reasons, no distinction is made between intersections with different flight levels or speeds when calculating cluster centres. This is a different level of abstraction.

The most important data for our approach are the intersections between the flights' routes. Because of the resulting very high amount of data, intersections are assumed to be similar if the distance between them is less than 0.1 NM. One representative is selected and the number of similar points stored with it.

5. Experimental setup

Within this section, the five scenarios based on three traffic samples are introduced and an overview of the simulation parameters, such as used flight samples, selected airspace area and observed flight levels, is given.

5.1. Scenarios

The goal of this paper is to prove the ability of the presented approach to build a route structure based on planned traffic data or demand data. To achieve this, a sequence of three traffic samples within the German airspace area based on planned traffic on 12th of July 2012 was created.

The first sample consists of a set of planned flight trajectories (no free routing). The goal of this planned sample is to investigate whether the approach presented here is able to create a main-flow system with comparable efficiency and similar routes to the current route system. Both systems are based on planned traffic data where the planned routes for the current system are a sequence of waypoints whilst the main-flow-based route is a sequence of intersections, respectively cluster centres. The efficiency of the created main-flow system in comparison to the current system is measured for each flight by calculating the main-flow route length as percentage of the originally planned route length and the similarity by applying the trajectory distance measure presented in Section 5.2.1. This scenario serves as a baseline for validating the ability to identify and emulate traffic streams.

EUROCONTROL simulations EUROCONTROL, 2005 have already shown the advantage of a combination of a route system for dense traffic areas and a free-route system for areas with less traffic. Taking this into account, two more traffic samples were created, whereby one represents free routing within the boundary of the German airspace area with entries and exits as planned and captured in historical data and the other consists of all flights where the great-circle trajectories from origin to destination move through the observed airspace part. Furthermore, for both free-routing samples, two different parameter sets were defined and tested, resulting in five scenarios.

The flight trajectories for all traffic samples are shown in Fig. 7. It is obvious that the trajectories for the planned traffic sample (left) are very similar, creating intersections which are very close together. Despite using the same entry and exit points, the traffic for the free-routing scenario is more widespread, but the flights of the great-circle traffic sample show the least structure and are

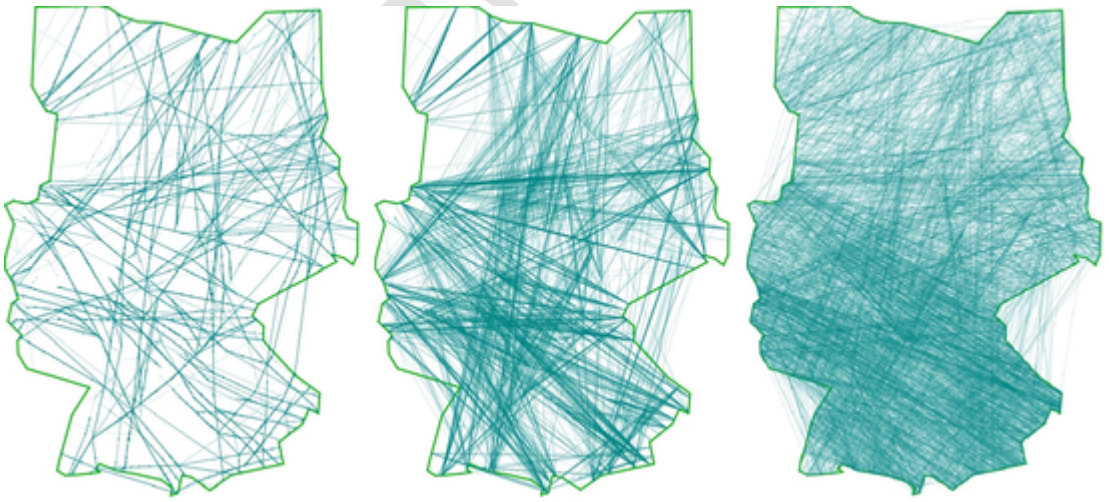

Fig. 7. Planned (left), free-route (centre) and great-circle route (right) trajectories as blue lines. The darker the colour, the more flights use a trajectory segment. (For interpretation of the references to colour in this figure legend, the reader is referred to the web version of this article.)

distributed the most. The resulting traffic is more unstructured due to the direct connections between origins and destinations. Because of the limited number of positions for start and end of flights (mainly airports), it is expected that there exists a hidden structure in the seemingly unstructured traffic.

The first traffic sample was selected from DDR2 data of EUROCONTROL (2018b) and restricted to flight level 320 and above (Table 1). For the free-routing traffic sample, all waypoints within the German airspace were removed and entry and exit points linked via a direct connection. The height and speed were determined based on the original route. For the great-circle routing sample, all routing points from flight level 100 and above were removed from their planned trajectory.

This trajectory part was then replaced by equidistant waypoints along the great-circle route for every flight. Whilst the height gradient was recalculated based on the original trajectory and applied to the new trajectory part, the speed was set to the average speed of the removed trajectory part. The original arrival and departure routes up to flight level 100 were retained in order to mirror arrival and departure structures. For the arrival part, time stamps have been adapted to the new travel time of the exchanged route part. These great-circle routes have then been used to determine new entry and exit points into the area under investigation. Some of the resulting great-circle routes no longer cross this area, resulting in a smaller traffic sample. For the calculation of the main-flow system, the time parameter is not considered because the focus lays on the creation of a main-flow system with its general traffic streams and the identification of necessary crossways between identified main flows.

5.2. Metrics

5.2.1. Trajectory distance

We use *the Symmetrized Segment-Path Distance* (SSPD) metric Besse et al., 2016 to compare the closeness of a planned flight trajectory to the generated reduced route. The *Segment-Path Distance* (SPD) is the average point-to-trajectory distance for all routing points of a trajectory G to the segments of a trajectory T (Fig. 8). SSPD is the average of SPD(G, T) and SPD(T, G).

5.2.2. Complexity

We aim to develop a complexity metric that reflects the influence of a structure in the form of a possible route system on potential controller workload for a given traffic situation. The metric has to cope with:

- Flights mostly lined up in a dominant flow (separated procedurally by altitude differences once applied).
- Dominant flows intersected by less frequented other flows.
- Traffic from various directions with similar intensity.
- Broad variability in usage of intersection points.

Various metrics defined in the literature measure ATM-related complexity ranging from single values to complexity plots based on diverse parameters. Prandini et al. (2011) give a good overview of various air traffic complexity measures and the relation to workload. The ACE working group on complexity also assessed several measures and defined a complexity measure that is applied in the yearly European ACE benchmarking reports EUROCONTROL, 2006. Most newer complexity measures commonly take some kind of metrics into account, evaluating traffic density, traffic patterns and traffic flows.

Here, we aim to assess the complexity of a possible route system rather than actual traffic flows. Nevertheless, some widely used aspects can be retained. We generate a complexity plot based on a cell size of 20 NM × 20 NM, as is used e.g. for the ACE benchmarking EUROCONTROL, 2006. The angle at which two routes meet defines potential horizontal interactions. Again as in EUROCONTROL, 2006, we use 15° as lower bound, others e.g. Gianazza (2007) use 20°. Route segments with an angle of 0 to 15 degrees

Table 1
Traffic samples.

	Traffic Sample 1	Traffic Sample 2	Traffic Sample 3
# Flights	4669	4669	3962
Traffic Type	Standard routing	Free routing	Great-circle routing above FL 100
Speeds	Planned	Original boundary entry/exit speed	Former average speed

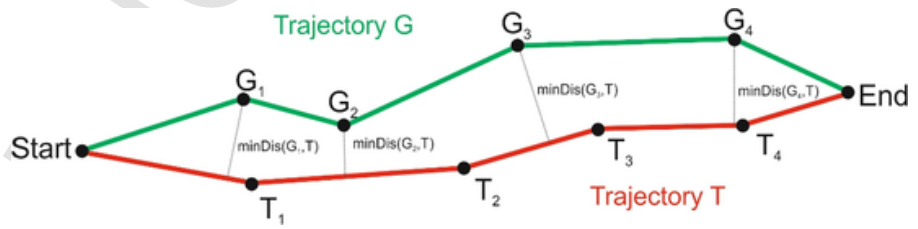

Fig. 8. Point-to-trajectory distances for routing points of trajectory G to segments of trajectory T. minDis(G_i, T) denotes the minimal point-to-segment distance of point G_i to trajectory T.

are handled as similar and of more than 15–180 as opposite (Fig. 9). When calculating an intersection between two route segments, the smaller angle is always used. To evaluate potential horizontal interactions of a route system, we take into account a frequency for the usage of particular route segments at intersection points.

Our complexity metric is based on the angle between links leading to or emerging from an observed cluster centre c. This metric is applied to two different application areas: intersections between free/direct routes and links from or to cluster centres (Fig. 10). In the first case, the angle between both lines can be calculated directly. In the second case, the intersection point is the cluster centre and a route segment moving through this cluster centre is not necessarily a straight line but may consist of any sequence of links connected to c. Furthermore, not all sequences of incoming and outgoing links are used in the flight sample.

Firstly, we associate a weight with the angle α between two links l_1 and l_2. This weight is defined as

$$w(\alpha) = \begin{cases} 10 & if\ 15 \le \alpha \le 165 \\ 1 & otherwise \end{cases} \tag{3}$$

Then, a complexity value cv for an intersection or a cluster center can be defined as follows.

Let point c be a cluster center and RS the set of all link sequences $\overline{l_i l_o}$ of incoming and outgoing links l_i and l_o for this cluster center and $n\left(\overline{l_i l_o}\right)$ the number of occurrences of this link sequence in all flights of the sample. The complexity factor of link $\overline{l_i^1 l_o^1} \in RS$ in combination with link $\overline{l_i^2 l_o^2} \in RS$ is defined as follows:

$$cf\left(\overline{l_i^1 l_o^1}, \overline{l_i^2 l_o^2}\right) = \left(w\left(\measuredangle\left(l_i^1, l_i^2\right)\right) + w\left(\measuredangle\left(l_i^1, l_o^2\right)\right) + w\left(\measuredangle\left(l_o^1, l_i^2\right)\right) + w\left(\measuredangle\left(l_o^1, l_o^2\right)\right)\right)/4 \tag{4}$$

In cases where a cluster is a start or end point of routes, Eq. (4) is adapted to the reduced number of link combinations. The usage frequency depends on whether the link sequences of a combination are equal:

$$uf\left(l^1, l^2\right) = \begin{cases} n\left(\overline{l_i^1 l_o^1}\right) * n\left(\overline{l_i^2 l_o^2}\right), & l^1 \neq l^2 \\ n\left(\overline{l_i^1 l_o^1}\right) * \left(n\left(\overline{l_i^2 l_o^2}\right) - 1\right), & l^1 = l^2 \end{cases} \tag{5}$$

The complexity value of a cluster is then defined as the sum over all complexity factors for all $\overline{l_i l_o} \in RS$ multiplied by the usage frequency of $\overline{l_i l_o} \in RS$ and divided by the sum of all usage frequencies:

$$cv(c) = \left(\sum_{l_1, l_2 \in RS} cf\left(\overline{l_i^1 l_o^1}, \overline{l_i^2 l_o^2}\right) * uf\left(l^1, l^2\right)\right) / \left(\sum_{l_1, l_2 \in RS} uf\left(l^1, l^2\right)\right) \tag{6}$$

The cells of a complexity plot are coloured in dependence on the sum of all complexity factors of all clusters in this cell in ten possible colours ranging from bright green to dark red.

In the case of free routing, the complexity factor of an intersection of two different routes (Fig. 10, left) is defined as $w(\measuredangle l_i^1, l_i^2)$. To generate the complexity plot, the complexity factors are summed up for each cell depending on an intersection's location.

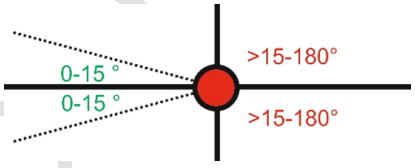

Fig. 9. Definition of similar and other direction between links (black lines).

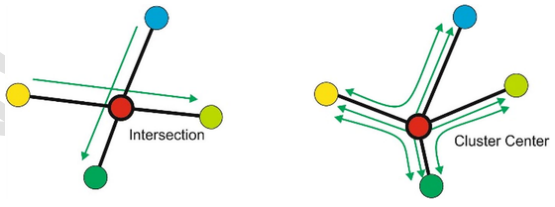

Fig. 10. Calculation of angles between intersecting lines (left) and cluster links (right), green arrows denote used directions. (For interpretation of the references to colour in this figure legend, the reader is referred to the web version of this article.)

5.3. Simulation parameters

Our research examines the question as to whether an adapted, more structured form of free routing would be able to combine the advantages of short trajectories with many intersections with the more structured, controllable form using predefined routing systems. Therefore, the length of the reduced flight trajectories in comparison to free-routing or planned trajectories is an important characteristic for the efficiency, as is the number, position and structure of the detected cluster centres, which represent the main-flow intersections (see Section 3.2). Therefore, two parameter sets are used for each of the two free-routing samples in order to analyse the influence of the selected set on the created system with respect to trajectory length and structure of cluster centres. One parameter set was selected with a focus on short flight trajectories and the other set for a combination of a low number of cluster centres whilst accepting slightly higher trajectory length.

Table 2 shows the DBSCAN parameters ϵ in NM and *minPts* (Section 2.2.1) selected to cluster the intersections as well as the entry and exit points on the boundary for all five scenarios. For the entry and exit points, three different sets were used for the different scenarios.

To select the parameter ϵ for a given *minPts* value, a so-called sorted k-dist graph has been used Ester et al., 1996. K-dist assigns each intersection to the distance to its k-nearest neighbour. This is the distance necessary to include k elements in the surrounding circle of the considered intersection. Subsequently, the intersections are sorted in descending order with respect to their k-dist values and plotted. Abrupt gradient changes indicate appropriate threshold values for the distance ϵ. All intersections on the left side of this threshold value are then defined as noise and those on the right side are cluster elements. An example for a sorted k-dist diagram for the intersections of scenario 1 with $k = 20$ is given in Fig. 11. Because many points are nearly identical, the k-dist values for many clusters are zero. The diagram (Fig. 11) was restricted to non-zero values for k-dist and therefore shows only the interesting part of the curve with the gradient change.

Table 2
Parameter sets for DBSCAN.

Objects clustered	Scenario	Traffic Sample	ϵ [NM]	*minPts* [# Points]	Compared with
Intersections	1	Planned Trajectories	0.5	20	Standard/ direct routes
	2	Free routing	0.5	20	Direct routes
	3	Free routing	1.5	100	
	4	Great-circle routing	0.8	50	Great-circle routes
	5	Great-circle routing	1.5	150	
Entry/Exit points	1,2,	Original Entry/Exit	2.0	3	–
	3	Original Entry/Exit	2.5	5	
	4,5	Great-Circle Entry/Exit	1.5	8	

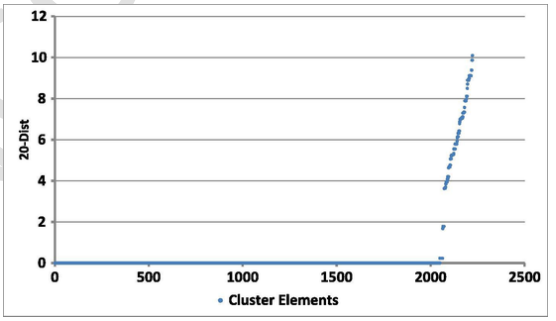

Fig. 11. Relevant part of the sorted 20-dist diagram for scenario 1.

To select appropriate parameters, several clustering tests with different values of k and associated ϵ in the range of 0.1 and 2.0 of the k-dist curve were carried out. The selected *minPts* values depend strongly on the data density and distribution. To create a route network for a dense traffic distribution on defined routes as for scenario 1, the *minPts* value has to be high enough (and the resulting ϵ low) to identify cluster centres. The intersections for the scenarios 2 and 3 are widespread and less dense, resulting in fewer intersection points within a larger airspace portion.

For the hill-climbing algorithm in step D.3 (point-balancing process, Section 3.2), 1000 incremental adaptations are created using a Gaussian distribution with mean 0 and variance 1 for x and y coordinates of the cluster centre for each cluster centre. Only solutions with a distance of less than or equal to 2.5 nautical miles around the original position are allowed.

The selected parameter sets for scenarios 3 and 5 (Table 2) are a compromise between a preference for a low number of cluster centres and a reasonable average trajectory length in comparison to the direct route. Nevertheless, the lower cluster number may lead to a higher complexity, caused by the dense traffic for several cluster centres. These preferences work against each other because a low number of cluster centres leads to fewer possibilities for the A* algorithm (Step C) to create a trajectory and therefore to an increase in trajectory length and more traffic using each cluster centre. This may exceed the capacity of these nodes with respect to controller workload.

6. Results

Within this section, the results for the three traffic samples described in Section 5 are presented, together with an overview of the computational efficiency for the different steps of this approach. The adapted and optimised main-flow systems are intermediate steps towards the resulting reduced main-flow system. Therefore, their results are presented for scenario 1 only to demonstrate the development of the main metrics during the calculation.

6.1. Computational efficiency

The computational efficiency in relation to the amount of handled data is an important factor and often a trade-off between accuracy and efficiency Sun et al., 2006. To gain efficiency, we reduce the amount of intersection data (Section 3.1). Therefore, intersections with a distance of less than 0.1 NM were defined as equal. Only one representative is used, together with the number of duplicates. As a result, the number of possible cluster elements decreased considerably in comparison to the number of intersections (Table 4).

The observed airspace was overlaid with a grid with square size $\epsilon \times \epsilon$ NM. Afterwards, each possible cluster element was assigned, together with the number of its duplicates, to the square $(x/\epsilon, y/\epsilon)$ to which its coordinates (x, y) belong. To create the ϵ-neighbourhood for a selected possible cluster element, only the elements within the grid cells surrounding the cell with the active element have to be considered. With these adaptations, the computation time for DBSCAN (step B, Section 3.2) decreased considerably, whilst the time needed for pre-processing the intersections (step A) increased with the number of intersections (Table 3). Computation times for step C depend strongly on the number of cluster centres, because the A* algorithm uses existing links between cluster centres as possible parts of the new trajectory. Step D includes the point-balancing functionality which also works on every identified cluster element.

As hardware, a workstation with an Intel® Xeon® E5-1630 v4 processor (4 kernels), 64 GB RAM and Windows 7 as operating system was used. The algorithms are implemented in Java.

6.2. Planned trajectories for the German airspace area

The first sample has been selected as a baseline for validation. The goal is to recreate the standard route system as closely as possible with a comparable efficiency by analysing planned flights.

Table 3
Computation times in seconds for the process Steps A to D (Section 3.2).

Scenario	Step A	Step B	Step C	Step D
1	128	22	58	1
2	13	25	1665	4
3	15	31	4	1
4	10	20	780	1
5	11	20	35	1

Table 4
Cluster structure data for scenario 1.

Scenario	Trajectory intersections	Different intersections	Adapted cluster centres	Reduced cluster centres	Percentage of noise
1	8,457,742	7252	2029	1425	0.18

Table 4 shows the general results for scenario 1. The very high number of trajectory intersections is caused by trajectories which are close together and therefore have a higher chance of intersecting with other trajectories. Furthermore, different flights use identical trajectory segments and thus common waypoints of these segments are identified as intersections. As a side effect, the number of different intersections is very low compared to the number of all intersections.

The number of cluster centres is reduced by more than 99% from adapted to reduced routes and the percentage of noise is very low. The traffic structure follows predefined standard flight routes and this leads to intersection hotspots which can be easily identified. Fig. 12 shows the cluster centres created in Step B and the cluster elements. Most clusters are small with a high number of (nearly identical) elements.

Therefore, it can be expected that the clusters are very dense. The cluster density $density(C)$ can be measured with the following equation Brisaboa et al., 2009:

$$density\,(C) = |C| \,/ \max\,\{\, d(x,y) | \, x,y \in C \,\} \tag{7}$$

with $d\,(x,y)$ = distance from x to y. $density(C)$ can be seen as the number of cluster elements per length unit. Fig. 13 shows the cluster density diagram for scenario 1. Due to the high number of duplicates, there are many clusters with low density values or even zero density. The few clusters on the left side have either a high number of elements or a very low maximal distance (below 1) and are therefore very dense.

The resulting adapted and reduced main-flow structures are presented in Fig. 14. They are similar but the reduced main-flow structure has fewer rarely used connections (thin lines). Furthermore, the number of cluster centres is reduced for the main flows.

Table 5 shows the major results for the reduced main-flow system of scenario 1. For each metric, the location parameters median, first and third quartiles are presented.

An important metric for evaluating the quality of the created main-flow system is the route length in comparison to the length of the planned trajectories. The comparison between planned and direct routes was included to demonstrate the quality of the planned route structure. The route length for the reduced system is given as a percentage of the planned trajectories. The median is very close to the planned routes and even the interquartile range (IQR) including 50% of the data between first and third quartile is very small. Therefore, the lengths are very similar. The third column shows the results of the SSPD metric focusing on the similarity of the trajectories. Again, the distances between both trajectory types are very low with a median of only 0.3 NM. Together, both results prove the ability of our approach to emulate a given route system. The fourth column shows the number of trajectories running through each cluster centre for the complete data sample (full day). This number can be used as an indicator for the expected controller workload to supervise these nodes. Furthermore, it can be used as an indication of safety, because the number of trajectories through a cluster centre influences the conflict probability for this point. With an interquartile range of 76, the expected workload will be very unequally distributed over the cluster centres, as indicated by Fig. 14.

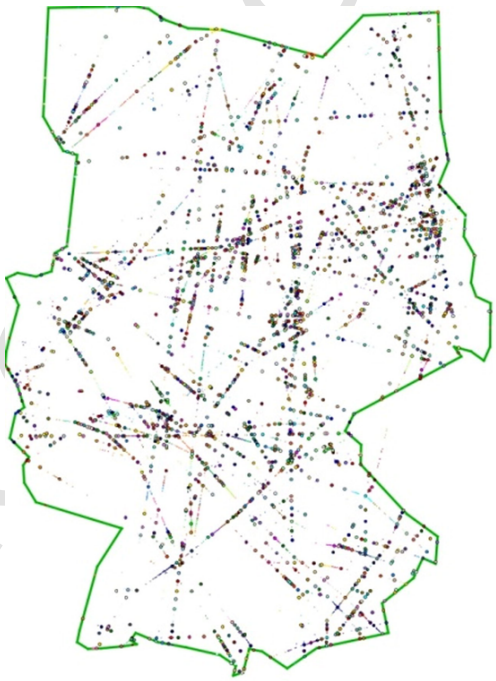

Fig. 12. Cluster elements and cluster centres for scenario 1.

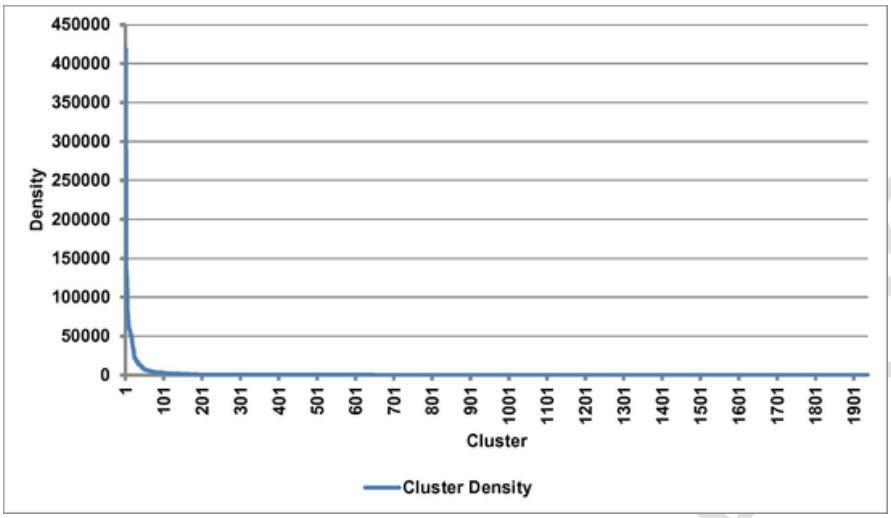

Fig. 13. Inner cluster density diagram for scenario 1.

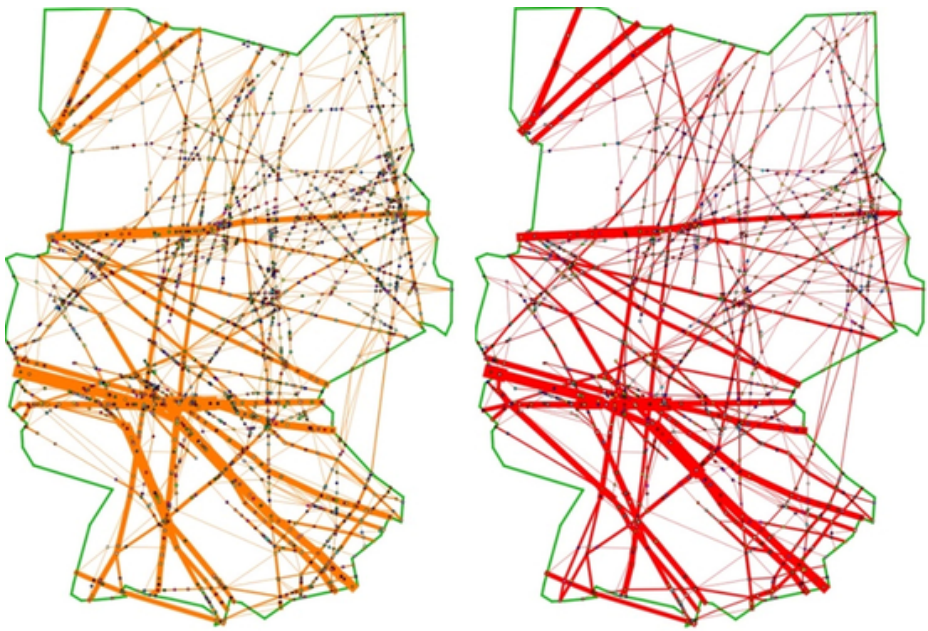

Fig. 14. Adapted (left) and reduced (right) main-flow system for scenario 1. Cluster centres marked by coloured circles. Line thickness depends on number of flights using a link. (For interpretation of the references to colour in this figure legend, the reader is referred to the web version of this article.)

Table 5
Main-flow key data for scenario 1.

	Route length planned relative to direct routes [%]	Route length reduced relative to planned routes [%]	SSPD [NM]	Number of trajectories per cluster centre[#]
Median	101.0	100.0	0.3	51
First Quartile	100.2	99.5	0.1	22
Third Quartile	102.9	100.2	0.8	98

The left side of Fig. 15 is a box plot showing the relation between the lengths of all trajectories and the original trajectories. The right side depicts the distribution of trajectories over cluster centres. Most of the lengths for adapted and reduced trajectories are very close to the original trajectory. The high values for the adapted trajectories are partly caused by repeated visits to the same

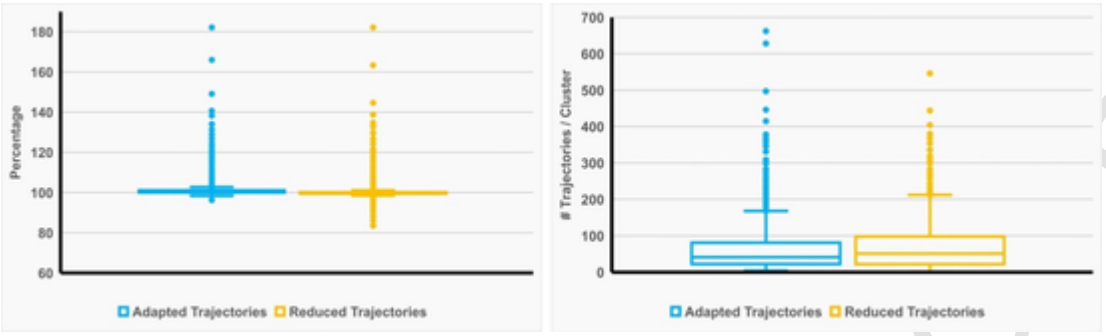

Fig. 15. Adapted and reduced route length as percentage of the planned route trajectory (left) and number of trajectories at each cluster centre (right) for adapted and reduced trajectories for scenario 1.

cluster centre, as shown in Fig. 3. Overall, there is a significant decrease of route length from adapted to reduced trajectories. The reduction of the number of cluster centres carried out in step D.1 increases the number of trajectories for the remaining cluster centres as well as median and IQR. Even the upper whisker (median plus 1.5 times the IQR) is higher for the reduced version, indicating that more cluster centres have a higher trajectory number. Altogether, the main-flow system that is based only on a traffic sample for one exemplary day is able to closely emulate the structure of the underlying route system.

6.3. Free routing within the German airspace area

Within this section, the results for scenarios 2 and 3 are presented. Here, the original boundary entry and exit points are maintained and the trajectory therein is substituted by a direct connection (Section 5.1). These scenarios are the consequent intermediate step towards general (great-circle) free routing picked up in scenarios 4 and 5.

Table 6 presents the main indicators of the cluster structure for both scenarios. The number of different intersections is in both cases higher than for scenario 1, due to the wider distribution of flight trajectories (Fig. 7, centre). The scenario parameters (Table 2) were selected with two different objectives regarding the main-flow system: The goal of scenario 2 is to adhere as closely as possible to the free-routing trajectories, whereas a low number of cluster centres is the intention of scenario 3. Table 6 validates that the number of cluster centres as well as the percentage of noise are significantly lower for scenario 3 than for scenario 2.

Fig. 16 illustrates this. The clusters of scenario 3 are larger and include elements with a higher distance. Since the number of cluster centres is already low for ACA, they can be hardly further reduced with RCA. The ability of scenario 2 to distinguish between close cluster centres is accompanied by a high number of cluster centres.

A closer look at the cluster density curves in Fig. 17 shows very low densities below 200 for both scenarios, but the peaks on the left side of the curves are higher for scenario 2. This shows that the lower noise value for scenario 2 is accompanied by clusters with a higher amount of elements. Only a few clusters have a very high density, indicating a high number of elements in relation to the maximum inner cluster distance. An example for such a cluster is the large orange area just below the centre of Fig. 16 (right) with 641 167 elements. For scenario 2, the cluster with the most elements is at the same location in dark green and has 123 000 elements.

For both scenarios, the reduced systems shown in Fig. 18 reflect the structure of the free-route trajectories, but in the case of scenario 2, there are more connections and it is dissected into many small links. The structure of the underlying traffic sample is visible with clearly identified main flows in both scenarios. Especially the reduced main flows of scenario 3 are restricted to the main directions of the underlying traffic sample, resulting in an increased trajectory length for flights having adapted boundary entries and exits. For scenario 2, the high number of links in areas through which the majority of routes pass ensures the possibility of staying close to the original free-route trajectory and of distributing flights more equally over the network. Nevertheless, the higher the number of cluster centres, the more complex the supervision of traffic for controllers.

Table 7 summarises further results of the main-flow system for both scenarios. As expected, all parameters for the route length are significantly lower for scenario 2 than for scenario 3, due to the very different amount of cluster centres. Together with the SSPD, it can be concluded that scenario 3 was less able to adjust the route structure to the given flight routes in a satisfying way. Due to the higher amount of cluster centres in scenario 2 (Table 6), the number of trajectories per centre is considerably lower than for scenario 3.

Table 6
Cluster-structure data for scenarios 2 and 3.

Scenario	Free-route intersections	Different intersections	Adapted cluster centres	Reduced cluster centres	Percentage of noise
2	1,941,831	112,679	8738	3603	7.9
3	1,941,831	112,679	968	804	6.6

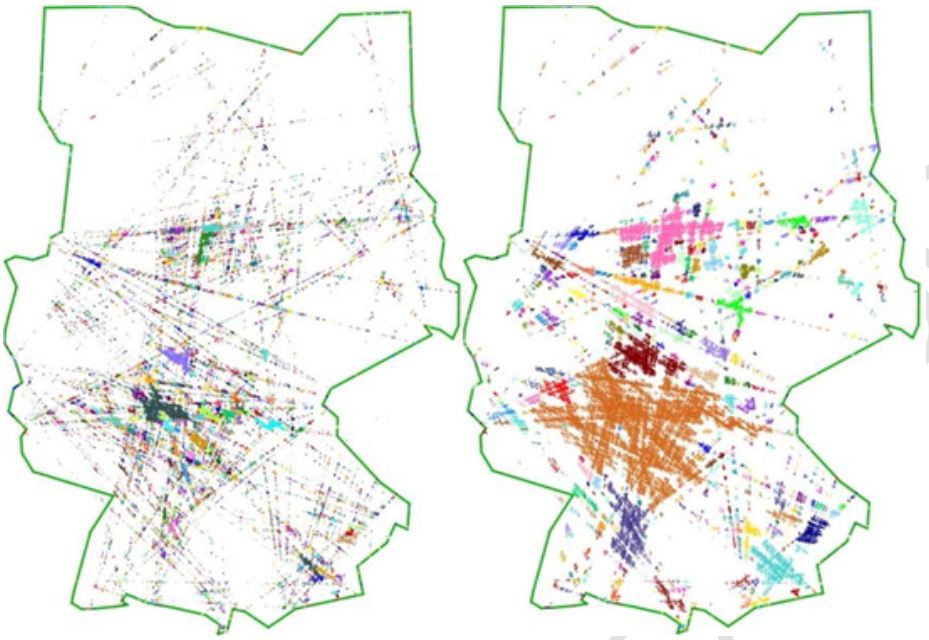

Fig. 16. Cluster elements for scenarios 2 (left) and 3 (right).

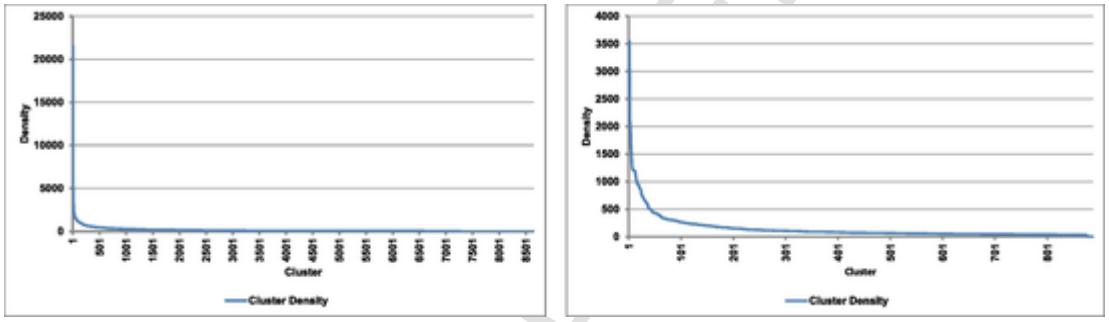

Fig. 17. Inner cluster-density diagram for scenarios 2 (left) and 3 (right).

The structural complexity of the intersections themselves is close to 10, indicating a highly irregular traffic structure with a low number of flights using the same flight directions at intersections. In contrast, the structural complexities of cluster centres are much better for both scenarios. With most flights on main flows and only a few flights crossing these main flows, the structural complexity decreases significantly in comparison to the complexity of intersections. For scenario 2 this is even more obvious, because crossing traffic is distributed on the main flows over several different cluster centres. Crossing traffic therefore has a smaller influence on the calculation of the structural complexity value than for scenario 3, where all crossing traffic uses the same cluster centre on a main flow. In addition, the IQR is higher in the case of scenario 3, indicating more variation in the structural complexity of the observed cluster centres. The reduced amount of clusters in scenario 3 and the resulting less complex main-flow system lead to a higher IQR than for scenario 2. With fewer incoming and outgoing route links for scenario 2, adverse flow directions are less probable.

The box plots presented in Fig. 19 confirm these results. The plots show the trajectory length in relation to the direct route length for both scenarios. Values below 100% indicate routes shorter than the original direct route, caused by replacing the boundary entry/exit points by cluster centres so that the new connection is shorter. For scenario 2, the lengths of the reduced trajectories are very close to the free-route trajectory. The interquartile range indicated by the size of the box is small. Together with the small SSPD (Table 7), this shows that the majority of trajectories are similar to corresponding direct connections.

For scenario 3, the interquartile range is higher and there are more outliers with a higher deviation from the median (Fig. 19). Also, the SSPD in Table 7 is higher for scenario 3. This shows that trajectories allocated to the main flows are short, but others are very long, caused by a lack of possible waypoints. Fig. 20 denotes the number of trajectories moving through each cluster centre. This value can be used to estimate the expected controller workload.

Due to the high number of cluster centres, these values are considerably lower for scenario 2. The low interquartile range shows that the expected workload is more uniformly distributed over the cluster centres than in scenario 3. High values of the interquartile

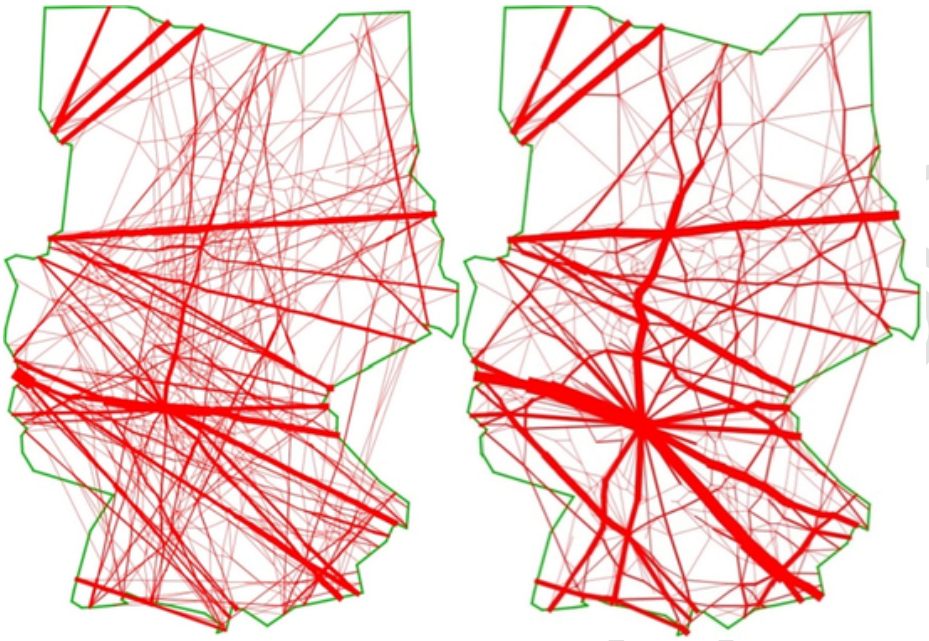

Fig. 18. Reduced main-flow systems for scenarios 2 (left) and 3 (right). Line thickness depends on number of flights using a link.

Table 7
Main-flow key data for scenarios 2 and 3.

Scenario		Route length relative to direct routes [%]	Number of trajectories per cluster centre [#]	Structural complexity intersections	Structural complexity cluster centres	SSPD [NM]
Scenario 2	Median	100.9	32	9.8	3.6	0.8
	First Quartile	100.2	16	9.7	2.6	0.3
	Third Quartile	102.2	59	9.9	4.5	1.8
Scenario 3	Median	103.8	57	9.8	4.6	2.5
	First Quartile	100.9	22	9.7	2.8	1.0
	Third Quartile	109.0	105	9.9	6.3	4.7

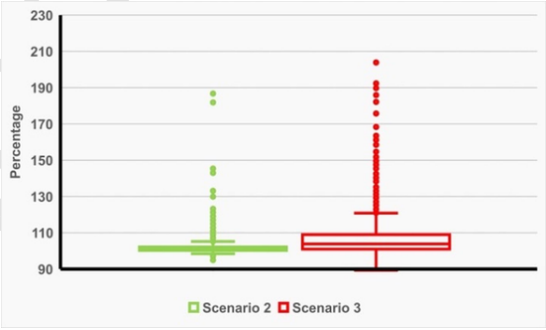

Fig. 19. Relation of route length to free-route trajectory length in [%] for reduced trajectories of scenarios 2 (green) and 3 (red). (For interpretation of the references to colour in this figure legend, the reader is referred to the web version of this article.)

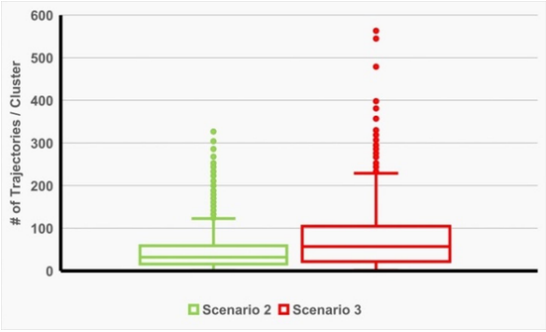

Fig. 20. Box plot with number of trajectories per cluster for scenarios 2 (green) and 3 (red). (For interpretation of the references to colour in this figure legend, the reader is referred to the web version of this article.)

range and the maximal values indicate that some cluster centres have a significantly higher amount of passing trajectories, which will make it more difficult for controllers to handle them.

Fig. 21 illustrates the average structural complexity on a grid with squares sized 20x20 NM. The left part shows the complexity of the intersections, the centre image illustrates the results of scenario 2 and the right of scenario 3. The trajectories (left) and reduced routes (centre and right) are included as blue lines. The left figure has only very few white (unused) squares, because the intersections are distributed over the whole area. The figure for scenario 3 to the right has the most unused areas, because the traffic is concentrated on a smaller number of cluster centres. Nevertheless, it is not necessary for an airspace controller to supervise the unused airspace of scenarios 2 and 3. For scenario 3, the main cluster centres with many connected links are red.

6.4. Great-circle routing for the German airspace area

Scenarios 4 and 5 are great-circle scenarios restricted to the German airspace area, see Section 5.1. As shown in Fig. 7, the traffic and, in turn, the intersections are widely spread. The number of total intersections in Table 8 (left column) gives a good impression of the problem complexity. The amount is lower than for scenarios 2 and 3, because of the wider distribution of traffic. The number of different intersections is three times as high. By applying the procedures to optimise and reduce the main-flow system, the num-

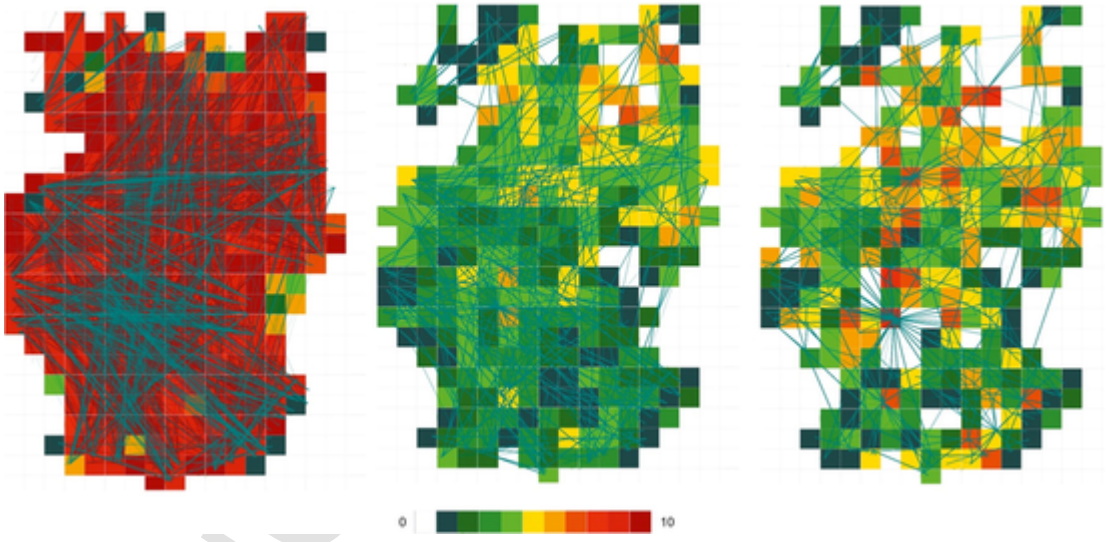

Fig. 21. Structural complexity. Intersections (left), cluster centres for scenario 2 (centre) and scenario 3 (right).

Table 8
Cluster-structure data for scenarios 4 and 5.

Scenario	Free-route intersections	Different intersections	Adapted cluster centres	Reduced cluster centres	Percentage of noise
4	1,392,404	356,159	4761	3686	37.8
5	1,392,404	356,159	1286	1184	37.4

ber of cluster centres was reduced to 3686, respectively 1184 clusters. This is a reduction of 22% for scenario 4 and only 8% for scenario 5. The low reduction for scenario 5 reveals that the adapted main flows already included only the most important centres. As expected, due to the traffic structure, the percentage of noise is very high in both scenarios.

In Fig. 22, the clusters are illustrated. Note that only few clusters in the northern part of the airspace are detected in both scenarios although both parameter sets are very different, see Section 5.3. Scenario 4 was able to detect several traffic streams indicated by cluster centres on a straight line.

The cluster density for scenario 4 is lower than for scenario 5 (Fig. 23), where the same amount of intersections is distributed to a lower number of clusters with a similar percentage of noise. The increase of the number of elements per cluster for scenario 5 was higher in relation to the inner cluster distance. The maximal number of cluster elements are 24 961 for scenario 4 and 59 269 for scenario 5 and therefore lower than for scenarios 2 and 3.

The RCA main-flow systems are shown in Fig. 24. In the southern part of the area, several promising main flows can be identified for scenario 4, together with many less-used links. The traffic structure is more visible in the case of scenario 5. The reduced main-flow structures are slightly different but they tend to have main flows in the same part of the airspace. The main-flow system of scenario 4 has a fine granularity, whereas scenario 5 combined less-frequented traffic streams to smaller main flows. With respect to trajectories, this is accompanied by an increase in trajectory length.

The results for the main-flow system are depicted in Table 9. As expected, the route length in relation to the direct routes' length is shorter for scenario 4 than scenario 5, due to the higher number of cluster centres. The same is the case for IQR. This shows that many routes received greater detours in scenario 5. This is underlined by the SSPD, which is also significantly higher for scenario 5.

The box plots in Fig. 25 show the trajectory lengths in more detail. There are outliers in scenario 5 for which the route length is three times as long as the corresponding direct route. Values below 100% are again caused by shifting entry and exit points towards their cluster centres. The amount of trajectories passing through a cluster centre (Fig. 26) is quite different for the observed scenar-

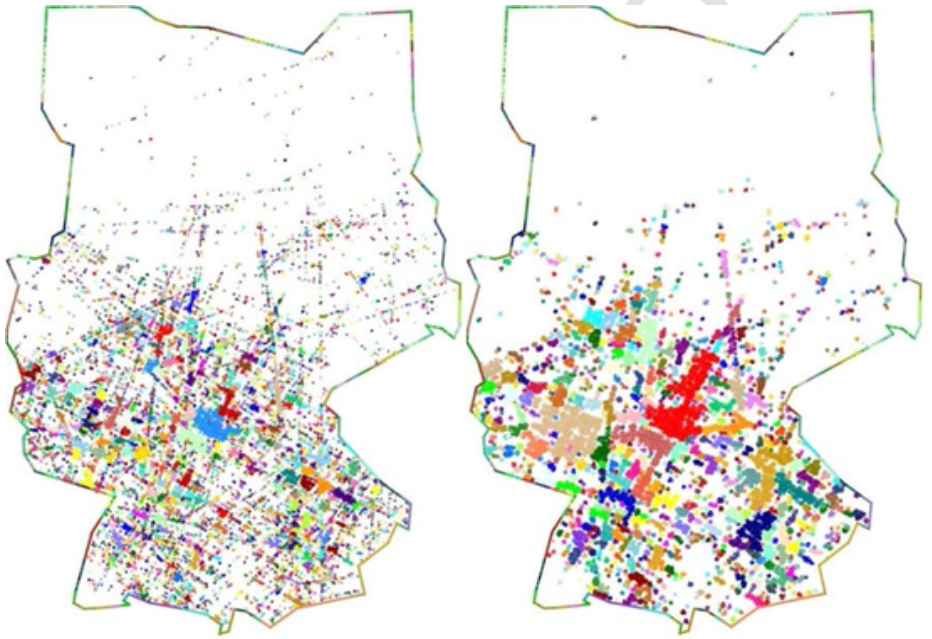

Fig. 22. Cluster elements for scenarios 4 (left) and 5 (right).

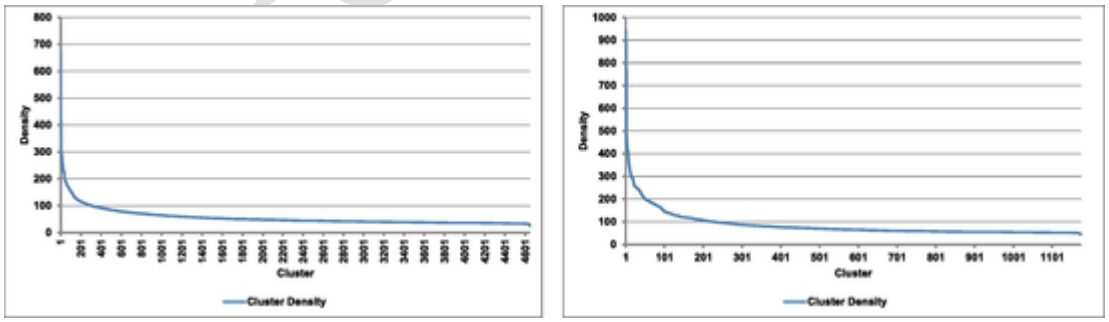

Fig. 23. Inner cluster-density diagram for scenarios 4 (left) and 5 (right).

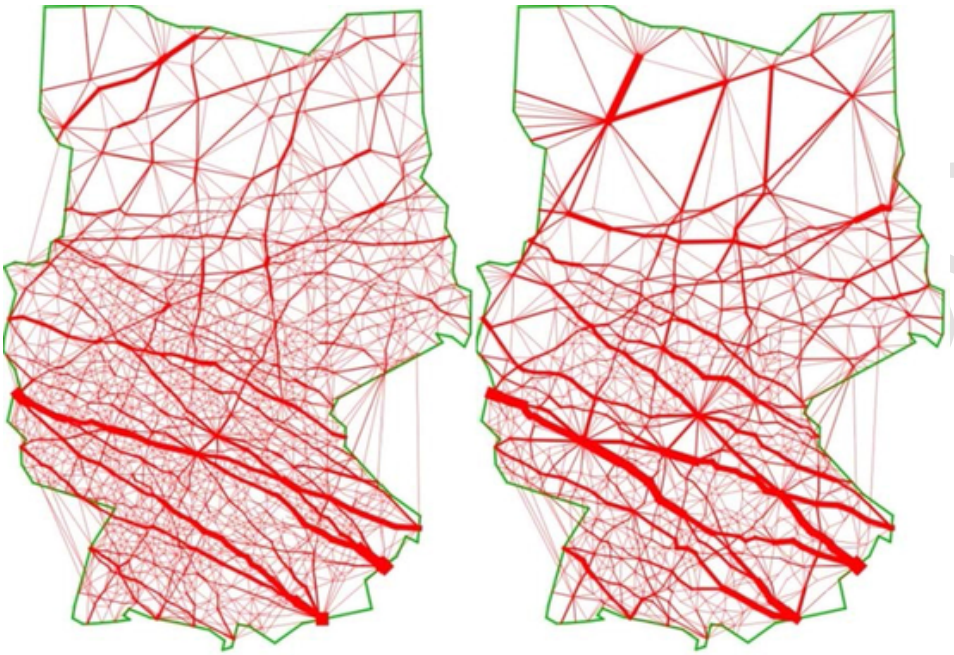

Fig. 24. Reduced main-flow systems for scenarios 4 (left) and 5 (right). Line thickness depends on number of flights using a link.

Table 9
Main-flow key data for scenarios 4 and 5.

Scenario		Route length relative to direct routes [%]	Number of trajectories per cluster centre [#]	Structural complexity of intersections	Structural complexity of cluster centres	SSPD [NM]
Scenario 4	Median	104.1	26	9.7	5.6	4.3
	First Quartile	101.9	12	9.6	5.0	2.6
	Third Quartile	107.6	47	9.8	6.3	7.0
Scenario 5	Median	106.5	42.5	9.7	6.5	5.9
	First Quartile	103.5	18	9.6	5.6	3.7
	Third Quartile	112.4	85	9.8	7.3	9.1

ios, due to the lower number of cluster centres for scenario 5. Furthermore, the IQR for the number of trajectories per cluster is significantly higher in the case of scenario 5, indicating an inhomogeneous distribution of flights over the cluster centres.

The reduction of cluster centres and, therefore, possible waypoints has led to a less balanced distribution of trajectories to cluster centres. The value for the third quartile of 85 raises the question as to whether the traffic will be distributed over the day in such a way that the controller will be able to handle it.

The values for the structural complexity of intersections are very high, caused by the traffic structure, and the complexity is nearly the same for all grid cells. This implies that all cells require the same monitoring attention. On the other hand, the values for the structural complexity of clusters are much lower and wider spread. There are cells which require supervision with a higher probability than others. The higher values of scenario 5 are again caused by the lower number of cluster centres, leading to more connected links and, therefore, penalised route-segment combinations. Examples are the cluster centres in the upper part of Fig. 27, right and the red cluster (Fig. 22) in the centre of the map. Particularly the last one also has a very high structural complexity and will be difficult to handle.

The structural complexity is presented for the grid cells in graphical form in Fig. 27. For the intersections, the structural complexity is high for the whole area. It varies between red (9) in the northern third and dark red (10) in the southern part of the air-

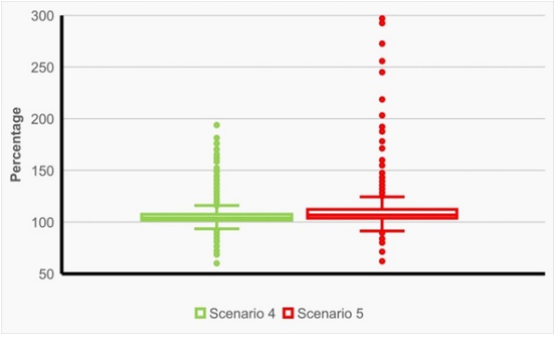

Fig. 25. Relation of route length to great-circle trajectory length in [%] for reduced trajectories for scenarios 4 (green) and 5 (red). (For interpretation of the references to colour in this figure legend, the reader is referred to the web version of this article.)

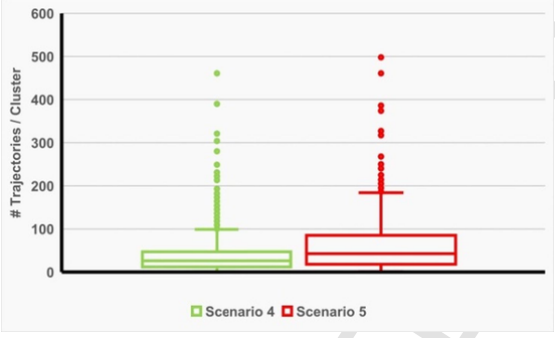

Fig. 26. Box plot with number of trajectories per cluster for scenarios 4 (green) and 5 (red). (For interpretation of the references to colour in this figure legend, the reader is referred to the web version of this article.)

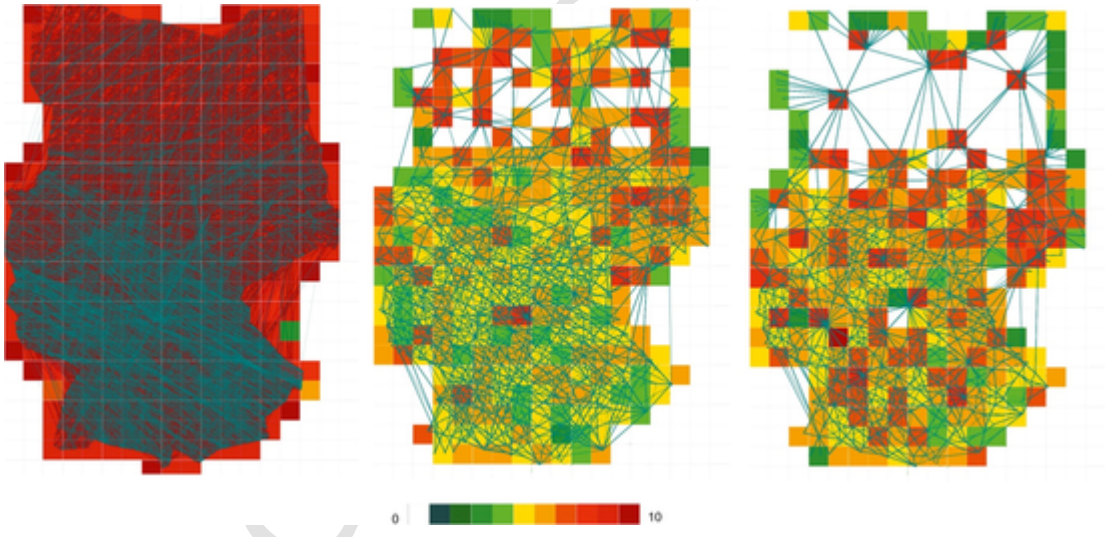

Fig. 27. Structural complexity: Intersections (left), cluster centres for scenarios 4 (centre) and 5 (right).

space, due to numerous intersections indicating unstructured traffic. This changed to values mainly between 3 (green) and 7 (orange) for the cluster centres. There are a few grid cells in red (9) or dark red (10), especially for clusters with many used link combinations. The green cells for scenario 4 mark areas where the traffic is distributed to several cluster centres and the main traffic is using the main-flow routes.

Nevertheless, taking the results for the median trajectory lengths presented in Fig. 25 into account, this approach has the ability to identify main flows even under adverse conditions. Furthermore, these two scenarios show that the results strongly depend on the selected set of simulation parameters. It is therefore necessary to find a compromise between the preference for a low number of cluster centres, an equally distributed number of trajectories per cluster centre and a low average trajectory length.

7. Discussion

The results presented in Section 6 show the possibility to develop an adapted, more structured form of free-route airspace using the intersections between all trajectories of the observed traffic samples. The presented approach is able to combine the advantages of short trajectories on the one hand with the more structured, controllable form using predefined flight routes on the other. The results also show that the further processing of the adapted trajectories by removing nodes and applying a pathfinding algorithm is useful and helpful in creating a system of easily useable main flows.

Three traffic samples have been presented: today's structured traffic for validation (scenario 1, Fig. 28, left), free routing within the boundary of the German airspace area (scenario 2, Fig. 28, centre) and great-circle routing (scenario 4, Fig. 28, right) to identify a main-flow structure. The results have shown that our approach is able to recognise diverse traffic structures using the intersections between trajectories. However, it was necessary to mark a high percentage of intersections as noise (37.8%) for scenario 4 compared to 0.2% for scenario 1 and 7.9% for scenario 2 in order to achieve an appropriate main-flow structure. Flights with intersections classified as noise are sent via cluster centres and therefore received a longer route compared to the great circle. The identified structures of scenarios 1 and 2 are very similar in spite of the different traffic scenarios. This confirms that today's traffic within the German airspace area often already uses direct routes. However, the main-flow structure for scenario 4 is quite different, as is the used traffic sample. Furthermore, the results for the trajectory lengths for scenario 2 are slightly closer to the direct routes than the planned routes. The IQR is even lower, indicating that the routes of scenario 2 are more often closer to the direct routes. Because of the completely different traffic scenario, it is not possible to compare the results of scenario 5 to the results of the direct route for scenario 1.

Fig. 28 represents the efficiency-related main results of Section 6. It is clearly visible that the main flows are very close to the underlying traffic for scenario 1 respective 2 and that the main flows for scenario 4 are located at and follow the higher-frequented areas. Even for this scenario, main flows at the same positions as for scenarios 1 and 2 are identified, especially in east-west direction. This gives the impression that the standard flight routes identified in scenario 1 are already close to the routes needed for a free-routing system. Reasons are the introduction of several free-routing areas in Europe and the increased assignment of direct routes by DFS Bentrup and Hoffmann, 2016. The resulting length of the trajectories for scenario 1 in relation to the planned trajectories of 101.2% and in relation to the direct routes for scenario 2 (100.9%) and scenario 4 (104.1%) demonstrate the ability to identify and emulate the course of traffic. These good results show that most trajectories receive an appropriate reduced trajectory whilst the remaining trajectories have to fly detours to reach their destination.

To assess the feasibility of a new approach, controller workload and safety are important factors for measuring the complexity of traffic. A simple workload measure is the number of airplanes in a defined airspace area (sector), for other measures see e.g. Gerdes et al., 2018. Here, the number of trajectories passing a cluster centre, together with the structural complexity, can be used to measure the expected controller workload and to assess the safety aspect. The more trajectories use the same cluster centre in an uncoordinated way, the higher the workload for controllers in supervising complex traffic situations. Scenario 4 needed 3686 cluster centres to approximate the used traffic sample with the main-flow system in comparison to 1425 for scenario 1 and 3603 for scenario 2. The more possibilities there are to compose a trajectory, the lower and more evenly distributed is the number of trajectories per cluster centre. Thus, a less dense distribution of traffic – as in the case of free routing – distributes the number of flights per cluster centre more uniformly and, in turn, the controller workload. With a median of 26, scenario 4 has the lowest value for trajectories using a cluster centre. This is not caused by the number of cluster centres, which is nearly the same as for scenario 2, but by

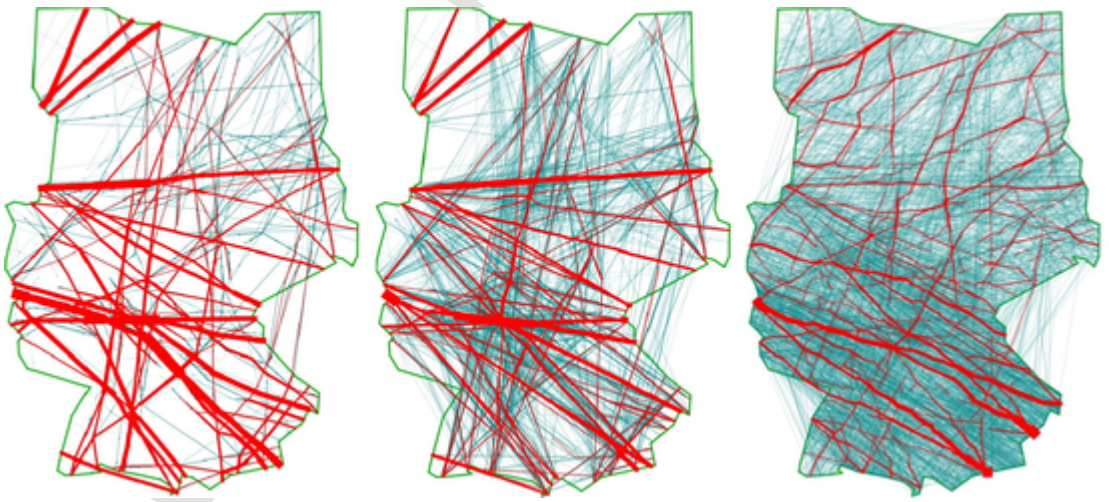

Fig. 28. Main-flow systems restricted to flows with more than 20 movements per link for scenarios 1 (left), 2 (centre) and 4 (right). Line thickness depends on number of flights using a link.

the distribution of traffic using the whole airspace. With a focus on the distance metric SSPD instead of complexity, scenario 1 has a value as high as 51 for this factor. Furthermore, the number of trajectories per cluster centre has to be seen in correlation to structural complexity, which is higher for scenario 4 than 2. The main-flow system created for scenario 4 is more complex than scenario 2, where most flights are lined up in a continuous sequence (main flows) with a low number of flights from other connected links. The traffic in scenario 4 is, however, more evenly distributed. In comparison, a concentration of traffic on predefined routes (as in scenario 1) may increase the number of trajectories per cluster centre but may decrease the structural complexity. A combination of free routing with a main-flow system as was applied to scenarios 2 and 4 resulted in a lower number of trajectories per cluster compared to scenario 1.

The presented results prove that this approach is able to create a suitable system based on a rarely structured traffic sample. Even for scenario 4, the created main-flow system follows the great-circle trajectories of this sample and ensures a maintainable level of structural complexity. This approach is therefore able to create a main-flow system for a great-circle scenario which is able to use the whole airspace, to create trajectories which are reasonably short in comparison to the direct connections, to distribute the traffic uniformly to a set of route intersections (cluster centres) and to maintain an appropriate level of structural complexity. All scenarios have shown that the use of intersections between trajectories allows the creation of a main-flow system adapted to a given traffic sample and that the reduced main flows may be used as a substitute for free-routing trajectories. Therefore, this approach is applicable to a general free-routing approach as well as to specialised free-routing areas or for identifying the actual route system.

8. Conclusions and outlook

The method of clustering intersections instead of complete flight trajectories described in this paper has proven to be a valid approach for identifying traffic streams and structuring free-route airspace. The presented scenarios demonstrated that the resulting main-traffic flows reflect the underlying traffic structure. In addition, the length of the resulting trajectories is comparable to the free-routing trajectories' length with an increase between 1.2% and 6.5% in median trajectory length. Although the number of cluster centres and therefore route segments for main flows is, in the case of free routing, higher than for today's system, this amount of segments is easier to monitor by air traffic controllers than a complete free-route airspace. This is indicated by lower values for the number of trajectories per cluster centre and reasonably low values of structural complexity. Furthermore, the necessity of regular free routing decreases when the airspace is used more efficiently by applying a main-flow system closer to the preferred direct connections between origin and destination. Altogether, the presented traffic-dependent, predefined route system combines successfully the advantages of free-route airspace with those of a predefined route system. We see this approach as an intermediate step between today's route system and the free-route airspace concept (great circle) as well as an alternative to free-route airspace in the case of heavily loaded airspace areas. Furthermore, with the described process, a fast identification of main flows was possible, meaning that it can be used for a time-dependent adaptation of the route system to changing traffic requirements.

In addition to the successful proof of concept, a clustering method based on intersections was developed which can be applied to other trajectory-clustering tasks. The actual approach does not consider varying flight levels. Instead, the focus is placed on the upper airspace in general. Nevertheless, it can be extended to support different main-flow systems for particular flight types such as intercontinental traffic on higher and district traffic on lower flight levels. In this case, different combinations of origins and destinations and lengths of flight trajectories may result in different main flows. Furthermore, a method was developed to evaluate the complexity of an airspace structure in relation to main flows crossed by less-frequented routes.

The approach presented here is a first step towards adapting free routing to a more structured and manageable route structure or adapting a route system dynamically to changing traffic patterns. Thus, open questions and research possibilities, especially on how to improve the main-flow structure, remain. One important point is whether a comparison of main flows for many days would allow the identification of common routes which could be seen as permanent. On the other hand, there may be temporary routes even for parts of a day (e.g. special morning traffic from Europe to US). Vidosavljevic et al. (2015) stated that the traffic complexity changes over the course of the day and this would influence the possible main-flow structure as well. Based on our findings, some future research questions are:

- Are there permanent main flows which can be identified for many days or periodical main flows which depend on the time of day?
- Is there really a strong necessity to introduce free routing if the main-flow pattern is mainly permanent over a longer period of time?
- Do airspace boundaries (e.g. between sectors) need to be adjusted to handle such a new main-flow system?
- What is the ideal number of cluster centres with respect to trajectory length and structural complexity?
- How will the air traffic controllers handle traffic organised with e.g. daily changing main flows?
- Which technical equipment is necessary to use a "predefined, dynamically changing" route system?

Typically, sectors are designed so that their boundaries are roughly perpendicular to main flows and that main intersection points are well within the sector. The third question addresses to what extent related characteristics are met when this new main-flow system is used with current sectors. Potentially, additional constraints have to be considered for the creation of main flows in order to cope with these requirements.

The focus of the actual approach is on the creation of a two-dimensional main-flow system based on a given traffic sample. In a first step, aircraft on opposing flight directions should be separated by different flight levels, following the semi-circular cruising levels, to include the vertical component.

Introducing main flows for free routing can be very promising, especially for restricted areas, since the positions of entry and exit points are limited and predefined by the route system outside the area under investigation. Nevertheless, the possibilities for improvements are smaller than for a great-circle scenario, due to the fixed entry and exit points and shorter flight times. Using a main-flow system based on free routing ensures an economically and ecologically efficient use of the airspace by using short, aircraft-preferred trajectories. Thereby, regular traffic patterns (e.g. east/west-bound traffic) as well as singular events (e.g. sector closure) can be covered.

One further important question is related to whether the removal of links with a low number of associated flights is possible without destroying the main-flow structure and without increasing the average trajectory length. In particular, cluster centres with a high number of connected links and therefore a high structural complexity may profit from this. Removing less-used segments may lead to a reduction in the number of cluster centres as well. This leads to a more clearly structured airspace route network. However, it is not clear, whether the removal of some links is able to decrease complexity without congesting the traffic network further, cf. the recent findings related to Braess's Paradox Cai et al., 2019. Taking into account the point-balancing carried out in step D.4 where all connected links influence the position of a cluster centre, removing some less-used links may lead to an advantageous position for many other trajectories. In addition, a reduced number of segments would increase the efficiency of the main-flow system, because air traffic controllers would have a lower number of route segments to supervise; on the other hand, this would increase the number of flights moving on each segment and through each cluster centre.

Acknowledgement

We would like to thank our reviewers for the constructive feedback and valuable suggestions which have influenced not only the paper but also our future work. This paper has benefitted considerably from their work and their professional method of handling the necessary critique.

Funding

This research did not receive any specific grant from funding agencies in the public, commercial or non-profit sectors.

Appendix A. Supplementary material

Supplementary data to this article can be found online at https://doi.org/10.1016/j.trc.2020.102633.

References

Airspace, 2017. The freedom of flight. Airspace Quarter 4, 12–15.

Ankerst, M., Breunig, M., Kriegel, H.-P., Sander, J. 1999. OPTICS: Ordering points to identify the clustering structure. In: ACM SIGMOD international conference on Management of data. Philadelphia, USA. https://doi.org/10.1145/304182.304187.

Basora, L., Morio, J., Mailhot, C. 2017. A Trajectory Clustering Framework to Analyse Air Trafic Flows. In: 17th Sesar Innovation Days. Belgrade, Serbia. – HAL Id : hal-01655747.

Bentrup, L., Hoffmann, M. 2016. Free Routing Airspace in Europe. In: 7th International Conference on Research in Air Transportation. Philadelphia, PA.

Besse, P, Guillouet, B, Loubes, J-M, Royer, F, 2016. Review & Perspective for Distance Based Clustering of Vehicle Trajectories. (IEEE, Hrsg.) IEEE Trans. Intelligent Transport. Syst. 3306–3317. doi:10.1109/TITS.2016.2547641.

Brisaboa, N.R., Luaces, M.R., Pedreira, O., Places, A.S., Seco, D., 2009. Indexing Dense Nested Metric Spaces for Efficient Similarity Search: In: Perspectives of Systems Informatics, 7th International Andrei Ershov Memorial Conference, PSI 2009, Novosibirsk, Russia, pp. 98–109. https://doi.org/10.1007/978-3-642-11486-1_9.

Cai, Q, Ma, C., Alam, S., Duong, V.N., Sridhar, B., 2019. Airway Network Flow Management using Braess's Paradox. In: 13th USA / Europe Air Traffic Management Research and Development Seminar. Vienna, Austria.

Chen, Z., Shen, H., Zhou, X., 2011. Discovering Popular Routes from Trajectories. In: IEEE 27th International Conference on Data Engineering. Hannover, Germany. https://doi.org/10.1109/ICDE.2011.5767890.

Churchill, A.M., Bloem, M., 2019. Clustering Aircraft Trajectories on the Airport Surface. In: 13th USA / Europe Air Traffic Management Research and Development Seminar, Vienna, Austria.

Cook, A, Tanner, G, Williams, V, Meise, G, 2009. Dynamic cost indexing – managing airline delay costs. J. Air Transport Manage. 15, 26–35. doi:10.1016/j.jairtraman.2008.07.001.

Delahaye, D., Puechmorel, S., Alam, S., Feron, E., 2018. Trajectory Mathematical Distance Applied to Airspace Major Flows Extraction. (L. N. Springer, Hrsg.) Lecture Notes in Electrical Engineering, Air Traffic Management and Systems III. - HAL Id : hal-01598864.

Ester, M, Kriegel, H-P, Sander, J, Xu, X, 1996. A Density-Based Algorithm for Discovering Clusters. KDD-96. AIAA.

EUROCONTROL, 2005. Air Traffic Freeway System for Europe. EUROCONTROL Experimental Centre, Brétigny-sur-Orge.

EUROCONTROL. 2006. Complexity Metrics for ANSP Benchmarking Analysis. ACE Working Group on Complexity.

EUROCONTROL. 2017. Free Route Airspace (FRA) Application in NMOC – Guidelines Version 1.1.

EUROCONTROL. 2018a. European Route Network Improvement Plan – PART 1 European Airspace Design Methodology - Guidelines. In: European Network Operations Plan 2018-2019/22.

EUROCONTROL. (2018b). DDR2 Reference Manual 2.9.5.

Gariel, M, Srivastava, A N, Feron, E, 2011. Trajectory Clustering and an Application to Airspace Monitoring. IEEE Trans. Intell. Transport. Syst. 12 (4), 1511–1524. doi:10.1109/TITS.2011.2160628.

Gerdes, I, Temme, A, Schultz, M, 2018. Dynamic airspace sectorisation for flight-centric operations. Transport. Res. Part C: Emerging Technol. 95, 460–480. doi:10.1016/j.trc.2018.07.032.

Gianazza, D., 2007. Airspace configuration using air traffic complexity metrics. In: 7th USA/Europe Air Traffic Management R&D Seminar. Barcelona, Spain.

Hart, P, Nilsson, N, Raphael, B, 1968. A Formal Basis for the Heuristic Fetermination of Minimum Cost Paths. (IEEE, Hrsg.) IEEE Trans. Syst. Sci. Cybernetics 2, 100–107. doi:10.1109/TSSC.1968.300136.

Hoekstra, J, 2001. Designing for Safety, the Free Flight Air Traffic Management Concept. NLR.

Hoekstra, J., Ruigrok, R., van Gent, R., 2000. Free Flight in a Crowded Airspace. In: 3rd USA/Europe Air Traffic Management R&D Seminar. Napoli, Italy.

ICAO. 2017. Free Route Airspace Design. In: Second Meeting of the Advanced Inter-Regional ATS Route Development Task Force (AIRARDTF/02), Astana, Kazakhstan.

ICAO EUR/NAT Office. 2018. Free Route Airspace (FRA) in ICAO EUR Region – Concept, Publication, Implementation, FAQs. In: ICAO / ACAC Civil / Military Workshop. Agiers, Algeria.

Krzyzanowski, M, 2013. Conflict Free and Efficient Flight Routes Planning in Free Route Airspace. (P. N. Warszaw, Hrsg.) Transport 277–285.

Lee, J.-G., Han, J., Whang, K.-Y., 2007. Trajectory clustering: a partition-and-group framework. In: SIGMOD '07. Beijing, China. https://doi.org/10.1145/1247480.1247546.

Marzuoli, A, Gariel, M, Vela, A, Feron, E, 2014. Data-Based Modeling and Optimization of En Route Traffic. J. Guidance, Control, Dynamics 37 (6), 1930–1945. doi:10.2514/1.G000010.

Mc Innes, L., Healy, J., 2017. Accelerated Hierarchical Density Clustering. In IEEE International Conference on Data Mining Workshops (ICDMW), (S. 33 - 42). New Orleans, USA. https://doi.org/10.1109/ICDMW.2017.12.

Mirkin, B, 1996. Mathematical Classification and Clustering. Kluwer Academic Publishers, Netherland ISBN 978-1-4613-0457-9.

Murca, M., Hansman, R., Balakrishnan, H., DeLaura, R., Jordan, R., Reynolds, T., 2016. Trajectory Clustering and Classification for Characterization of Air Traffic Flows. In: 16th AIAA Aviation, Technology, Integration and Operations Conference. Washington, D.C. https://doi.org/10.2514/6.2016-3760.

Prandini, M, Piroddi, L, Puechmorel, S, Brázdilová, S L, 2011. Toward air traffic complexity assessment in new generation air traffic management systems. IEEE Trans. Intelligent Transport. Syst. 12 (3), 809–810. doi:10.1109/TITS.2011.2113175.

Ratcliffe, S, 2001. Free-flight in europe, problems and solutions. J. Navigation 54 (2), 213–221. doi:10.1017/S0373463301001229.

Sridhar, B., Grabbe, S., Sheth, K., Bilimoria, K., 2006. Initial study of tube networks for flexible airspace utilization. In: AIAA Guidance, Navigation, and Control, Conference and Exhibit, Keystone, Colorado, AIAA-2006-6768.

Sunil, E, 2019. Analyzing and Modeling Capacity for Decentralized Air Traffic Control. TU Delft.

Sunil, E., Hoekstra, J., Ellerbroek, J., Bussink, F., Vidosavljevic, A., Delahaye, D., Aalmoes, R., 2016. The Influence of Traffic Structure on Airspace Capacity. In: ICRAT2016 - 7th International Conference on Research in Air Transportation. Philadelphia, United States. - HAL Id: hal-01333624.

Sun, D., Yang, S.D., Strub, I,Bayen, A., Sridhar, B., Sheth, K., 2006. Eulerian Trilogy. In: AIAA Guidance, Navigation and Control Conference and Exhibit. Keystone, Colorado. https://doi.org/10.2514/6.2006-6227.

Vidosavljevic, A., Delahaye, D., Sunil, E., Bussink, F., Hoekstra, J., 2015. Complexity Analysis of the Concepts of Urban Airspace Design for METROPOLIS Project. In: EIWAC. Tokyo. - HAL Id: hal-01234078.

Vlachos, M., Kollios, G., Gunopulos, D., 2002. Discovering Similar Multidimensional Trajectories. In: 18th International Conference on Data Engineering. https://doi.org/10.1109/ICDE.2002.994784.

von Luxburg, U, 2007. A tutorial on spectral clustering. Statist. Computing 4, 395–416. doi:10.1007/s11222-007-9033-z.

Xue, M, Kopardekar, P, 2009. High-capacity tube network design using the hough transform. J. Guidance, Control Dynamic 32, 788–795. doi:10.2514/1.40386.

Yousefi, A, Zadeh, A N, 2013. Dynamic allocation and benefit assessment of NextGen flow corridors. Transport. Res. Part C: Emerging Technol. 33, 297–310. doi:10.1016/j.trc.2012.04.01610.2514/6.2006-6768.

Yuan, G, Sun, P, Zhao, J, Li, D, Wang, C, 2017. A review of moving object trajectory clustering algorithms. (Springer, Hrsg.) Artif. Intell. Rev. 47 (1), 123–144. doi:10.1007/s10462-016-9477-7.

Glossary

$\measuredangle l_i, l_{io}$: :Angle between links l_i and l_o
ACA: :Adapted Connection Array
C_{cl}: :Set of cluster centers connected to a selected cluster center p
cv(c): :Complexity value of cluster center c
DBSCAN: :Density-Based Spatial Clustering of Applications with Noise
dist(p,c): :Euclidian distance between cluster centers p and c
ϵ: :Distance parameter for DBSCAN Algorithm
IQR: :Inter quartile range
minPts: :Minimum number of points to form a cluster
n_i: :Number of cluster centers for $i \in \{A(dapted), O(ptimized), R(educed)\}$
n_{pc}: :Number of flights using the connection between cluster center p and c
$n\left(\overline{l_i l_o}\right)$: :Number of occurrences of the link sequence $\overline{l_i l_o}$ in all flights
NM: :Nautical Mile
OCA: :Optimized Connection Array
RCA: :Reduced Connection Array
$S_{EL}(c)$: :Set of segment combinations entering and leaving a selected cluster center c
SSPD: :Symmetrized Segment-Path Distance
$w(\alpha)$: :Weight characterizing the angle between two links